Chronic hyperprolactinemia evoked by disruption of lactotrope dopamine D2 receptors impacts on liver and adipocyte genes related to glucose and insulin balance

Guillermina María Luque,[1]* Felicitas Lopez-Vicchi,[1]* Ana María Ornstein,[1] Belén Brie,[1] Catalina De Winne,[1] Esteban Fiore,[2] Maria Inés Perez-Millan,[1] Guillermo Mazzolini,[2] Marcelo Rubinstein,[3] and Damasia Becu-Villalobos[1]

[1]*Instituto de Biología y Medicina Experimental, Consejo Nacional de Investigaciones Científicas y Técnicas, Buenos Aires, Argentina;* [2]*Laboratorio de Terapia Génica, Instituto de Investigaciones en Medicina Traslacional (IIMT-CONICET), Universidad Austral, Buenos Aires, Argentina; and* [3]*Instituto de Investigaciones en Ingeniería Genética y Biología Molecular, CONICET, and Departamento de Fisiología, y Biología Molecular y Celular, Facultad de Ciencias Exactas y Naturales, University of Buenos Aires, Argentina*

Luque GM, Lopez-Vicchi F, Ornstein AM, Brie B, De Winne C, Fiore E, Perez-Millan MI, Mazzolini G, Rubinstein M, Becu-Villalobos D. Chronic hyperprolactinemia evoked by disruption of lactotrope dopamine D2 receptors impacts on liver and adipocyte genes related to glucose and insulin balance. *Am J Physiol Endocrinol Metab* 311: E974–E988, 2016. First published November 1, 2016; doi:10.1152/ajpendo.00200.2016.—We studied the impact of high prolactin titers on liver and adipocyte gene expression related to glucose and insulin homeostasis in correlation with obesity onset. To that end we used mutant female mice that selectively lack dopamine type 2 receptors (D2Rs) from pituitary lactotropes (lacDrd2KO), which have chronic high prolactin levels associated with increased body weight, marked increments in fat depots, adipocyte size, and serum lipids, and a metabolic phenotype that intensifies with age. LacDrd2KO mice of two developmental ages, 5 and 10 mo, were used. In the first time point, obesity and increased body weight are marginal, although mice are hyperprolactinemic, whereas at 10 mo there is marked adiposity with a 136% increase in gonadal fat and a 36% increase in liver weight due to lipid accumulation. LacDrd2KO mice had glucose intolerance, hyperinsulinemia, and impaired insulin response to glucose already in the early stages of obesity, but changes in liver and adipose tissue transcription factors were time and tissue dependent. In chronic hyperprolactinemic mice liver *Prlr* were upregulated, there was liver steatosis, altered expression of the lipogenic transcription factor *Chrebp*, and blunted response of *Srebp-1c* to refeeding at 5 mo of age, whereas no effect was observed in the glycogenesis pathway. On the other hand, in adipose tissue a marked decrease in lipogenic transcription factor expression was observed when morbid obesity was already settled. These adaptive changes underscore the role of prolactin signaling in different tissues to promote energy storage.

insulin; carbohydrate-responsive element-binding protein; sterol regulatory element-binding protein-1c; glucokinase; lipogenesis

THE ACTIONS OF PROLACTIN go far beyond its well-established role in lactation and pregnancy. It is involved in behavior, migrations, water and electrolyte balance, growth, development, immune regulation, and gonadal suppression, and strong evidence points to prolactin as a metabolic hormone (27, 33).

A large-scale tissue array method has identified several tissues that respond acutely to prolactin administration (42), including those that participate in metabolic regulation, such as liver, pancreas, adipose tissue, and brain, and concordantly, prolactin receptors (PRLR) are present in these tissues (13, 24, 45, 51, 61). On the other hand, prolactin and *Prlr* knockout mice do not exhibit a prominently altered metabolic phenotype (although there is lack of lactation and altered fertility in females) (41), indicating that many of the reported metabolic actions of prolactin are redundant or overlap with other physiological effectors. Nevertheless, understanding the role of prolactin becomes relevant in explaining many symptoms and manifestations that occur in prolactin overproduction, such as during pharmacological psychiatric treatments or in patients with prolactinomas.

The liver is a complex organ with multifaceted functions and paramount importance in glucose metabolism. It participates in maintaining long-term energy stores by conversion of carbohydrates to fat. Enzymes involved in these pathways are regulated by posttranslational mechanisms and respond to availability of nutrients and hormone levels. Long-term exposure of the liver to high levels of insulin and glucose results in alterations in these key enzymes. Insulin increases glycogen stores and lipogenesis (15, 71) and inhibits gluconeogenesis and glucose secretion (15) partially by induction of glucokinase (64).

In the synthesis of fatty acids, two important transcription factors participate regulating genes that encode enzymes for glucose metabolism or lipogenesis in the liver: sterol regulatory element-binding protein-1c (SREBP-1c) and carbohydrate-responsive element-binding protein (ChREBP). Both transcription factors may coordinately or independently regulate de novo lipogenesis and are differentially regulated by insulin and glucose (39, 74). *SREBP-1c* expression is stimulated by insulin via a phosphatidylinositol 3-kinase pathway (48), downregulates phosphoenolpyruvate carboxykinase, an enzyme involved in liver gluconeogenesis, and stimulates glucokinase which is involved in glycolysis and lipogenesis (21, 30). ChREBP, also fundamental in de novo lipogenesis in the liver (38, 72), is not directly stimulated by insulin but requires glucose phosphorylation via glucokinase to activate the expression of glycolytic and lipogenic genes (14, 37). It has been shown that *Chrebp* overexpression in liver induces hepatic

Table 1. *Primers used for real-time PCR*

Gene	Strand	Primer Sequence (5′–3′)	Source
Adiponectin	Sense	ATCCTGGCCACAATGGCACA	Primer Blast
	Antisense	CAAGAAGACCTGCATCTCCT	
Atgl	Sense	AGGACAGCTCCACCAACATC	Primer Blast
	Antisense	TGGTTCAGTAGGCCATTCCT	
Chrebp	Sense	TCGATCCGACACTCACCCA	Primer Blast
	Antisense	CCAGGCTCTCCAGATGGCGT	
Cyclophilin	Sense	TTCTTCATAACCACAGTCAAGACC	Primer Blast
	Antisense	ACCTTCCGTACCACATCCAT	
Fas	Sense	AAGTTGCCCGAGTCAGAGAA	Primer Blast
	Antisense	CGTCGAACTTGGAGAGATCC	
Ghr	Sense	CCAACTCGCCTCTACACCG	Primer Blast
	Antisense	GGGAAAGGACTACACCACCTG	
Glucokinase	Sense	CCGTGATCCGGGAAGAGAA	Primer Blast
	Antisense	GGGAAACCTGACAGGGATGAG	
Glucor	Sense	CGGGACCACCTCCCAAA	Primer Blast
	Antisense	CCCCATAATGGCATCCCGAA	
Gys2	Sense	CCAGCTTGACAAGTTCGA	Primer Blast
	Antisense	ATCAGGCTTCCTCTTCAG	
Hsl	Sense	TCTGCTGGCCCCTGACA	Primer Blast
	Antisense	AGAGCGCAAGCCACAAGGT	
Lpl	Sense	CCCTACAAAGTGTTCCATTACCAA	Primer Blast
	Antisense	TTGTGTTGCTTGCCATCCTCA	
*Prlr**	Sense	CACAGTAAATGCCACGAACG	Primer Blast
	Antisense	GGCAACCATTTTACCCACAG	
Prlr-l	Sense	CTGGGCAGTGGCTTTGAAG	Primer Blast
	Antisense	CCAAGGCACTCAGCAGTTCT	
Prlr-s1	Sense	CCTGCATCTTTCCACCAGTTC	Primer Blast
	Antisense	GGGAAGTCAACTGGAGAATAGAACA	
Prlr-s2	Sense	CCTGCATCTTTCCACCAGTTC	Primer Blast
	Antisense	TTTTCAAGTTGCTCTTTGTTGTGAA	
Prlr-s3	Sense	CCTGCATCTTTCCACCAGTTC	Primer Blast
	Antisense	GATCCACCTTGTATTTGCTTGGAG	
Srebp-1c	Sense	CAGCGGCCCTGAGGGTCAAA	Primer Blast
	Antisense	TGCATGGCAAGAGGCACCGA	

Atgl, adipose triglyceride lipase; *Chrebp*, carbohydrate-responsive element-binding protein; *Fas*, fatty acid synthase; *Ghr*, growth hormone receptor; *Glucor*, glucocorticoid receptor; *Gys2*, glycogen synthase 2; *Hsl*, hormone-sensitive lipase; *Lpl*, lipoprotein lipase; *Prlr*, prolactin receptor. *PRLR primers will potentially amplify 4 different Prlr mRNAs (if expressed): Prlr-l, Prlr-s1, Prlr-s2, and Prlr-s3.

steatosis (6), and high levels of liver *Chrebp* are found in obese mice (63). Nevertheless, ChREBP overexpression generates beneficial lipid signals that dissociate hepatic steatosis from insulin resistance, which positions ChREBP-regulated genes as therapeutic targets in the treatment of obesity-related diabetes (16, 37).

An effect of prolactin on liver gene expression is inferred by high *PRLR* mRNA levels found in hepatocytes (10, 13, 51), and within the liver prolactin activates numerous signaling pathways (42) and growth-related or -unrelated genes (7, 62, 70).

Prlr mRNA has also been documented in adipocytes, deducing a regulatory role for prolactin also in adipose tissue (46, 76). It participates in adipogenesis and adipocyte differentiation (18, 27), inhibits adiponectin (2), lipid protein lipase expression (59), and activity (46), and has been described to stimulate (29, 73) or inhibit (8) leptin. Prolactin enhances the expression of master genes of adipogenesis (52), and lack or *Prlr* in mice impairs parametrial, abdominal, and subcutaneous adipose tissues (19) and protects mice from high-fat diet-induced obesity (3). These metabolic actions are adaptive in pregnancy and lactation, physiological periods during which prolactin promotes fat deposition and mobilization, respec-

tively, to ensure optimal nutrition for the offspring (27). In humans, pathological hyperprolactinemia as in patients bearing prolactinomas may induce weight gain (28, 58).

Nevertheless, opposite functions have also been proposed for prolactin in adipogenesis. For example, a small reduction in retroperitoneal fat mass was found in transgenic mice that overexpress prolactin (45), abdominal adipose tissue is decreased during lactation (20), and prolactin has been found to suppress malonyl-CoA expression, suggesting that it inhibits lipogenesis (54). Therefore, the role of prolactin in adipocyte function is far from being settled.

Adipocyte SREBP-1c is involved in the regulation of genes associated with lipid metabolism, although its role in this tissue has not been clearly ascertained (4). On the other hand, adipocyte ChREBP is involved in de novo lipogenesis and is expressed at lower levels than in liver (37).

Finally, prolactin is also involved in pancreatic islet cell biology. It stimulates insulin expression and release, β-cell expansion (9, 27, 68), STAT5 tyrosine phosphorylation (42), and glucose transporter 2 (GLUT2) expression, and therefore, it promotes glucose entry into the β-cells (60), consistent with the presence of *Prlr* mRNA in islet cells (57). The effects of prolactin on glucose homeostasis during pregnancy promote glucose transfer to the fetus, and these peripheral actions of prolactin on metabolic homeostasis are reinforced by its action at the central nervous system.

But although prolactin is considered a metabolic hormone, its role on liver and adipose tissue gene expression, and particularly the expression of transcription factors involved in lipogenesis, has not been described. In a previous work, we showed that chronic high prolactin levels in 11-mo-old female mice that selectively lack dopamine type 2 receptors (D2Rs) from pituitary lactotropes (lacDrd2KO) (55) are associated with increased body weight beginning at 5 mo of age (59). In correlation, marked increments in fat depots, adipocyte size, serum triglycerides, and nonesterified fatty acid levels were found, a metabolic phenotype that intensified with age. Furthermore, 7-mo-old female lacDrd2KO mice had glucose intolerance but a preserved glucose response to insulin (59). Therefore, we have used this experimental model to study the role of high-prolactin titers on liver and adipocyte gene expression related to glucose and insulin homeostasis and in

Table 2. *PCR conditions for different genes*

Gene	Denaturation	Annealing	Extension
Adiponectin	95°C for 30 s	61°C for 1 min	72°C for 30 s
Atgl	95°C for 15 s	55°C for 20 s	72°C for 20 s
Chrebp	95°C for 20 s	60°C for 1 min	60°C for 1 min
Cyclophilin	95°C for 30 s	61°C for 1 min	72°C for 30 s
Fas	95°C for 15 s	55°C for 20 s	72°C for 20 s
Ghr	95°C for 20 s	60°C for 1 min	60°C for 1 min
Glucokinase	95°C for 20 s	60°C for 1 min	60°C for 1 min
Gr	95°C for 30 s	61°C for 1 min	72°C for 30 s
Gys2	95°C for 20 s	60°C for 1 min	60°C for 1 min
Hsl	95°C for 15 s	58°C for 20 s	72°C for 20 s
Lpl	95°C for 15 s	58°C for 20 s	72°C for 20 s
*Prlr**	95°C for 30 s	61°C for 1 min	72°C for 30 s
Prlr-l	95°C for 30 s	61°C for 1 min	72°C for 30 s
Prlr-s1	95°C for 30 s	61°C for 1 min	72°C for 30 s
Prlr-s2	95°C for 30 s	61°C for 1 min	72°C for 30 s
Prlr-s3	95°C for 30 s	61°C for 1 min	72°C for 30 s
Srebp-1c	95°C for 15 s	60°C for 1 min	60°C for 1 min

correlation with the development of hyperprolactinemia and obesity. To that end, we used lacDrd2KO mice of two developmental ages, 5 and 10 mo. At the first time point, obesity is not evident and body weight is marginally increased, although mice are hyperprolactinemic, whereas at 10 mo there is a 136% increase in gonadal fat and a 36% increase in liver weight due to lipid accumulation (59). Our present data highlight adaptive changes in chronic hyperprolactinemia that are associated with glucose intolerance, hyperinsulinemia, and impaired insulin response to glucose, which are already evident in early stages of obesity, and underscore the role of prolactin signaling in different tissues to promote energy storage.

MATERIALS AND METHODS

Animals. Mice lacking expression of D2Rs in pituitary lactotropes were generated by crossing $Drd2^{loxP/loxP}$ mice (5) with transgenic mice expressing *Cre* recombinase driven by the mouse prolactin promoter [Tg(Prl-cre)^{1Mrub} ; see Ref. 55] for two generations. Tissue specificity of *Cre* expression in Tg(Prl-cre)^{1Mrub} transgenic mice was analyzed by real-time PCR, and *Cre* mRNA levels were highly expressed in the pituitary and very low or almost absent in the hypothalamus, liver, kidney, ovary, and lung (59). Functional Cre recombinase activity was evaluated in the pituitary, and it was present in most prolactin-producing cells of the anterior pituitary in a highly selective manner, as described (55). LacDrd2KO and their $Drd2^{loxP/loxP}$ control littermates were congenic to C57BL/6J ($n = 10$).

Breeding pairs of female $Drd2^{loxP/loxP}$ and male $Drd2^{loxP/loxP}$.Tg-(Prl-cre) mice were used to generate $Drd2^{loxP/loxP}$(control) and $Drd2^{loxP/loxP}$.Tg(Prl-cre) (lacDrd2KO) littermates, which were included in each experiment. Mice of mixed genotypes were housed in groups of four or five in a temperature-controlled room, with lights on at 0700 and off at 1900, and had free access to tap water and laboratory chow except where indicated.

Because in male mice there was a marginal increase in prolactin levels and no differences in body or pituitary weight, fat mass depots, or food intake (59), we used female mice in our experiments.

Mice were euthanized by decapitation at defined ages. Sera were collected for cholesterol, triglycerides, and insulin measurements. Liver, adipose tissue, pancreas, and adrenals were processed for real-time PCR or immunohistochemistry, as detailed below.

All experimental procedures were carried out according to guidelines of and approved by the Institutional Animal Care and Use Committee of the Instituto de Biología y Medicina Experimental, Buenos Aires, Argentina (in accordance with the Animal Welfare Assurance for the Instituto de Biología y Medicina Experimental, Office of Laboratory Animal Welfare, National Institutes of Health, no. 5072-01).

Fasting and refeeding. Female lacDrd2KO and $Drd2^{loxP/loxP}$ mice at 5 or 10 mo of age were housed individually and fasted for 12 h, with the laboratory chow removed at 1900. Body weight was registered before and after fasting. After 12 h of fasting, one group was refed for 1 h (refed group), whereas the other one was fasted for an additional 1 h (fasted group). Finally, both groups were euthanized and samples collected.

Glucose tolerance test. Glucose tolerance test (GTT) was performed in conscious female lacDrd2KO and $Drd2^{loxP/loxP}$ mice at 5 and 10 mo of age. Briefly, after overnight fasting (8 h), intraperitoneal (ip) glucose solution (2 mg/g body wt) was administered. Blood glucose levels (2 μl of blood obtained from the tail of each mouse) were measured at 0, 15, 30, 60, and 120 min after glucose injection with a hand-held glucose monitor (Dex-II; Bayer).

Glucose-stimulated insulin secretion. Eight-hour-fasted 5- and 10-mo-old female mice were used. Tail blood glucose levels were measured before (0 min) and 30 min after glucose ip administration (3

mg/g). Serum samples were immediately obtained by centrifugation at 3,000 rpm for 10 min and stored at −20 C. Insulin secretion levels were assessed by a sensitive mouse insulin ELISA kit as described below.

Insulin ELISA. Mouse serum insulin levels were assessed by a sensitive mouse insulin ELISA kit (Crystal Chem, Chicago, IL), following the manufacturer's instructions. Aliquots of 5 μl of serum were used in duplicate. The lower limit of the assay sensitivity was 0.1 ng/ml.

Intraperitoneal insulin tolerance test. Five- and 10-mo-old mice were fasted for 2 h and then injected ip with human insulin (Humulin, 1 U/kg body weight; Eli Lilly, Toronto, ON, Canada). Tail blood glucose levels were measured 0, 15, 30, 60, and 120 min thereafter with a hand-held glucose monitor (Dex-II; Bayer).

Serum lipid profile. Triglycerides and total cholesterol were measured by Trinder colorimetric assay in 30 μl of diluted serum. The dilution was made with saline solution.

Prolactin RIA. Aliquots (10 μl) of serum obtained by decapitation of 5- or 10-mo-old mice were used to assay prolactin by RIA using a kit provided by the National Institute of Diabetes and Digestive and Kidney Diseases [Dr. A. F. Parlow, National Hormone and Pituitary Program (NHPP), Torrance, CA]. Results are expressed in terms of mouse prolactin standard RP3. Intra- and interassay coefficients of variation were 7.2 and 12.8%, respectively.

Hepatocyte culture. Hepatocytes were isolated from adult male 5-mo-old $Drd2^{loxP/loxP}$ mice, as described previously (17). Briefly, the liver was washed with washing buffer (Hanks' balanced salt solution) and digested with collagenase V (Sigma-Aldrich) by in situ perfusion. Then, liver cells were collected, centrifuged at 200 *g* for 10 min, washed, and plated in DMEM-F-12 supplemented with 10% FBS (Invitrogen) at a density of 2.5×10^4 cells/cm². After 3 h, medium was replaced. Two days after plating, hepatocytes were incubated for 6, 12, and 24 h with DMEM as a control or DMEM supplemented with 100 or 200 ng/ml prolactin (recombinant ovine prolactin from NHPP). The concentrations used were selected from Hartwell et al. (31). Cells were then collected in TRIzol reagent (Sigma-Aldrich) for total RNA extraction and real-time PCR analysis, as described below.

RNA extraction and cDNA synthesis. Gonadal adipose tissue and liver samples from $Drd2^{loxP/loxP}$ and lacDrd2KO were obtained and processed for recovery of total RNA using TRIzol reagent (Invitrogen, Carlsbad, CA). The RNA concentration was determined on the basis of absorbance at 260 nm, its purity was evaluated by the ratio of absorbance at 260/280 nm (>1.8), and its integrity was evaluated by agarose gel electrophoresis. RNAs were kept frozen at −80°C until they were analyzed. RNA (1 μg) was reversed transcribed in 20 μl of volume in the presence of 10 mM $MgCl_2$, 50 mM Tris·HCl (pH 8.6), 75 mM KCl, 0.5 mM deoxy-NTPs, 4 mM DTT, 0.5 μg oligo(dT)$_{15}$ primer (Biodynamics, Buenos Aires, Argentina), and 20 U of MMLV reverse transcriptase (Epicenter, Madison, WI). The reverse transcriptase was omitted in control reactions; the absence of PCR-amplified DNA fragments in these samples indicated the isolation of RNA that was free of genomic DNA.

Real-time PCR. Measurements were performed as described previously (25). Sense and antisense oligonucleotide primers were designed on the basis of the published cDNA or by the use of PrimerBlast (http://www.ncbi.nlm.nih.gov/tools/primer-blast/). Oligonucleotides were obtained from Invitrogen. The sequences are described in Table 1.

Briefly, the reactions were performed by kinetic PCR using TAQurate GREEN Real-Time PCR MasterMix (9.4 μl containing 10 mM Tris·HCl, 50 mM KCl, 3 mM $MgCl_2$, 0.2 mM deoxy-NTPs and 1.25 U *Taq* polymerase), 100 ng of cDNA, and 0.3 μM primers in a final volume of 10 μl. After denaturation at 95°C for 15 min, the cDNA products were amplified with 40 cycles. Cycle conditions (denaturation, annealing, and extension) for each gene are detailed in Table 2, and optical reading stage was performed at 80°C for 33 s. The accumulating DNA products were monitored by the ABI 7500 sequence detection system (Applied Biosystems,

Foster City, CA), and data were stored continuously during the reaction. The results were validated on the basis of the quality of dissociation curves (25) generated at the end of the PCR runs by ramping the temperature of the samples from 60 to 95°C while continuously collecting fluorescence data. Product purity was confirmed by agarose gel electrophoresis. Each sample was analyzed in duplicate. Relative gene expression levels were calculated according to the comparative cycle threshold (C_T) method. Normalized target gene expression relative to cyclophilin was obtained by calculating the difference in C_T values, the relative change in target transcripts being computed as $2^{-\Delta C_T}$. To validate the comparative C_T method of relative quantification, the efficiencies of each target and housekeeping gene amplification (endogenous cyclophilin) were measured and shown to be approximately equal.

Insulin RIA. Forty milligrams of pancreatic tissue were homogenized in 1 ml of ice-cold acidic alcohol solution (12.5% vol/vol HCl + 87.5% vol/vol ethanol) and incubated for 1 h at 4°C.

Samples were centrifuged at 800 g for 10 min at 4°C, and 100 μl of the supernatant was neutralized with 0.855 M Tris, to later determine insulin concentration by RIA. Protein content of samples was previously identified by Qubit Quant it protein assay kit (Invitrogen, Buenos Aires, Argentina), following the manufacturer's instructions, and RIA was performed with 50 ng of total protein. A specific insulin RIA was used as described previously (26), using human insulin for iodination and standard (Beta Laboratories, Buenos Aires, Argentina) and guinea pig anti-mouse insulin antibody (Sigma). The minimum detectable concentration was 0.002 ng/ml, and the intra- and interassay coefficients of variation were 6.8 and 9.1%, respectively.

Immunohistochemistry. Pancreases from 5-mo-old animals were fixed in formalin and embedded in paraffin. Immunohistochemistry was performed the using avidin-biotin peroxidase method, as described previously (47). Each immunohistochemical assay included negative controls, replacing the primary antibody with PBS. Antibodies for insulin (polyclonal guinea pig anti-insulin antibody, 1:200
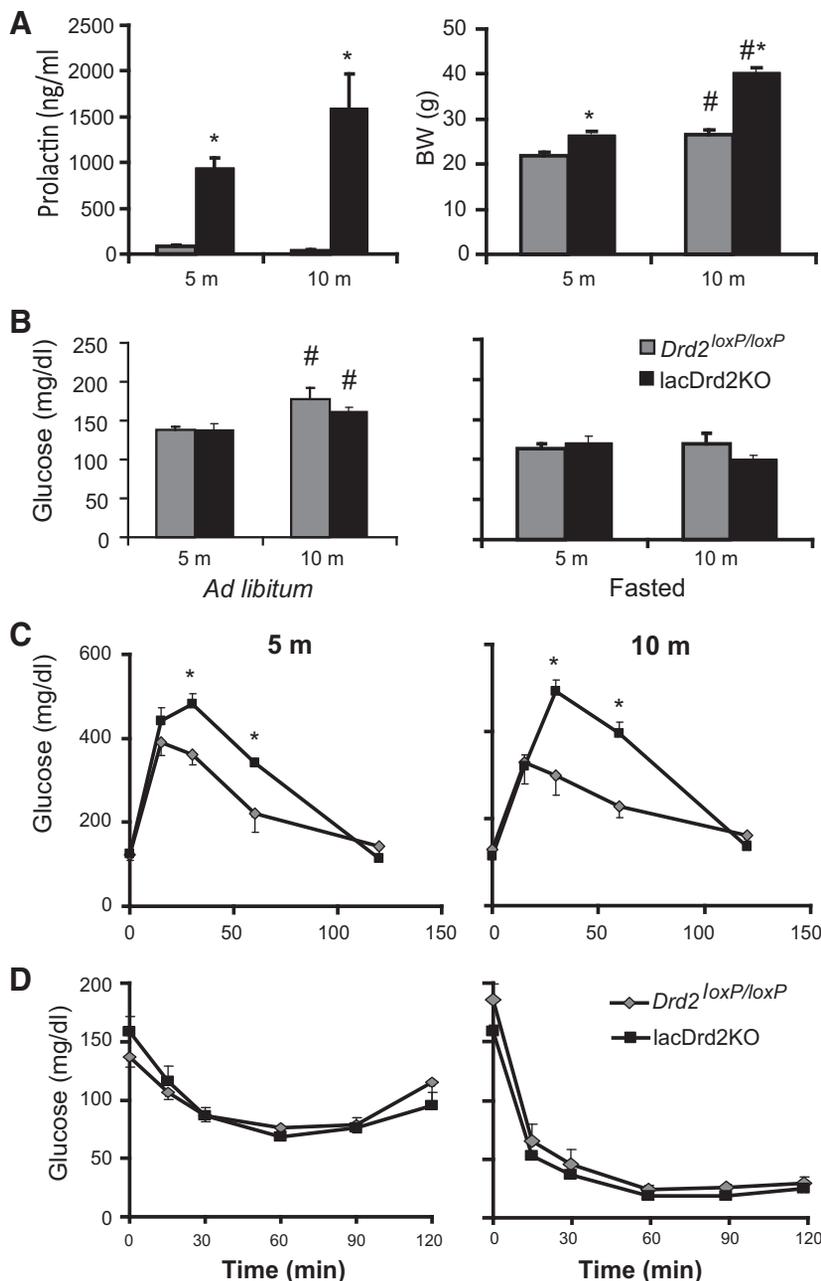

Fig. 1. High-serum prolactin, body weight, and glucose intolerance in lacDrd2KO female mice. *A, left*: serum prolactin levels (ng/ml) in ad libitum 5- and 10-mo-old female mice; $n = 10$ for each group. *$*P < 0.0001$ vs. age-matched mice. *A, right*: body weight in ad libitum 5- and 10-mo-old female mice; $n = 10$ for each group. *$*P < 0.001$ vs. *Drd2^{loxP/loxP}* age-matched mice; *$#P < 0.01$ vs. 5-mo-old genotype-matched mice. *B*: glucose levels (mg/dl) in the ad libitum condition (*left*) and after an 8-h fast (fasted; *right*) in 5- and 10-mo-old female *Drd2^{loxP/loxP}* and lacDrd2KO mice; n (ad libitum) = 5 and 7 (5 mo) and 5 and 5 (10 mo), and n (fasted) = 6 and 6 (5 mo) 7 and 8 (10 mo) for *Drd2^{loxP/loxP}* and lacDrd2KO mice, respectively. *$#P < 0.05$ vs. 5 mo genotype-matched mice. *C*: intraperitoneal glucose tolerance test (2 mg/g) in fasted *Drd2^{loxP/loxP}* and lacDrd2KO female mice [$n = 9$ and 9 (5 mo) and 4 and 6 (10 mo) *Drd2^{loxP/loxP}* and lacDrd2KO mice, respectively]. Two-way ANOVA with repeated-measures design. *$*P < 0.05$ vs. time-matched *Drd2^{loxP/loxP}* mice. *D*: insulin tolerance test in 5- and 10-mo-old *Drd2^{loxP/loxP}* and lacDrd2KO females. Mice were injected with 1 U/kg body wt human insulin, and blood glucose was measured at different times; no significant differences were found; $n = 13$ and 12 and 6 and 7 for 5- and 10-mo-old *Drd2^{loxP/loxP}* and lacDrd2KO female mice, respectively.

dilution; Abcam, Cambridge, MA) and glucagon (rabbit anti-gluca-gon, 1:200 dilution; Santa Cruz Biotechnologies, Santa Cruz, CA) were used. Appropriate secondary antibodies were chosen. Samples were counterstained with hematoxylin and mounted with permanent mounting medium.

Morphometric analysis. Pancreatic digital images were captured using a ×5 or ×40 magnification objective, a Zeiss Axiostar Plus microscope, and a Canon PowerShot G6 digital camera. To determine total pancreas area, the necessary images covering all the tissue with ×5 magnification were taken. Images of each islet were captured using ×40 magnification. Morphometric analysis was performed with the aid of ImageJ software (National Institutes of Health). The number of islets (defined as insulin-positive aggregates of ≥20 μm in diameter) was scored and used to calculate the islet numerical density (no. of islets/cm² tissue). Islets <5,000 μm² in size were defined as small and those >5,000 μm² as medium to large, and they were expressed as percentage of islets in each group. Mean islet size was calculated as the ratio of the total islet area to the total islet number on the sections. The relative areas occupied by islets and β-cells were also calculated as the ratio of islet or insulin-positive cell area to the total tissue area on the entire section, respectively. Counting the number of cells that showed insulin and glucagon staining in relation with total nuclei in islets (hematoxylin counterstaining), we determined the percentage of β- and α-cells, respectively. Data were calculated from three sections of each pancreas, representing the entire pancreas for each animal (head, body, and tail). Approximately 70–120 islets/section were analyzed. Six and seven animals were studied per genotype (Drd2^{loxP/loxP} and lacDrd2KO, respectively).

Hepatic glycogen content. Twenty to 25 mg of hepatic tissue was collected (the exact tissue weight was registered) from 5- and 10-mo-old female mice. Samples were incubated with 400 μl of 30% KOH in a boiling bath for 20 min. After the samples were cooled, 50 μl of a saturated solution of sodium sulfate (5%) was added. Ethanol (50%) was used to precipitate glycogen. A 0.15% Antrona (Merck Millipore) solution was added, and after 20 min of incubation at 90°C the samples were measured at 620 nm of absorbance (Multiskan, Thermo Scientific ELISA lector). Gycogen standard (Sigma) was used to perform calibration curves.

Statistical analysis. Results are expressed as means ± SE. The differences between means were analyzed by the unpaired Student's *t*-test (in the case of only 2 groups). Two-way ANOVA with repeated-measures design was used to analyze GTT, insulin tolerance test, glucose-stimulated insulin secretion, and the effect of prolactin on hepatocytes in vitro. Two-way ANOVA for independent measurements was used to analyze gene mRNA expression, glucose, and insulin levels (for the effects of: experimental condition × genotype, experimental condition × age, or genotype × age). Post hoc Tukey's test was employed when necessary. Percentages were analyzed by chi-square test. $P < 0.05$ was considered significant. Parametric or nonparametric comparisons were used as dictated by data distribution.

RESULTS

Glucose intolerance in 5- and 10-mo-old lacDrd2KO and Drd2^{loxP/loxP} female mice. Prolactin levels and body weight were increased at 5 and 10 mo of age in lacDrd2KO mice compared with age-matched Drd2^{loxP/loxP} mice (Fig. 1A), but body weight differences between genotypes were greater at 10 mo. Basal glucose levels were similar between genotypes at 5 and 10 mo in ad libitum-fed or fasted females (Fig. 1B). At 10 mo of age in the ad libitum condition, both genotypes had higher glucose levels than at 5 mo (Fig. 1B). Glucose intolerance after 2 mg/g glucose ip injection was evident in 5- and 10-mo-old lacDrd2KO mice (Fig. 1C) compared with Drd2^{loxP/loxP} mice, whereas no differ-

ences were found in glucose response to administration of 1 U/kg insulin (Fig. 1D).

Increased serum and pancreatic insulin levels in 5- and 10-mo-old lacDrd2KO females compared with Drd2^{loxP/loxP} control mice. LacDrd2KO female mice at 5 and 10 mo of age were hyperinsulinemic in the ad libitum condition (Fig. 2A), and in fasted lacDrd2KO mice there was a strong tendency toward higher insulin levels ($P = 0.057$ lacDrd2KO vs. Drd2^{loxP/loxP} mice; Fig. 2B). This correlated with increased insulin content in pancreas from lacDrdKO compared with Drd2^{loxP/loxP} mice at 5 and 10 mo of age both in ad libitum ($P = 0.000043$, lacDrd2KO vs. Drd2^{loxP/loxP} mice; Fig. 2C) and fasted conditions ($P = 0.000040$, lacDrd2KO vs. Drd2^{loxP/loxP} mice; Fig. 2D).

Pancreas sections were analyzed by immunohistochemistry in 5-mo-old mice. There was an increase in the relative β-cell area in pancreatic tissue as well as in the percentage of β-cell fraction within islets (Fig. 3, A and D, and Table 3), and even though islet number or density was similar in both genotypes (Fig. 3B) there was shift from small (<5000 μm²) to medium-large (>5,000 μm²) islets in lacDrd2KO compared with Drd2^{loxP/loxP} mice (Fig. 3, C and D). In concordance, percentage of islet area, mean β-cell size, and the ratio of insulin to glucagon immunoreactive areas were increased in lacDrd2KO mice (Table 3).

Impaired insulin response to glucose administration. Despite the increased pancreatic insulin concentration, in vivo insulin response to glucose administration (3 mg/g body wt) was im-
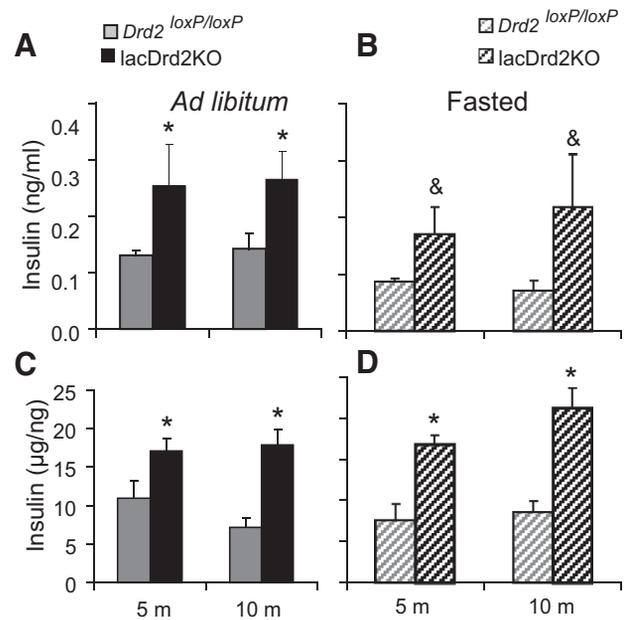

Fig. 2. Hyperinsulinemia in lacDrd2KO female mice. *A* and *B*: insulin levels (ng/ml) in the ad libitum condition (*A*) and after an 8-h fast (*B*) in 5- and 10-mo-old female Drd2^{loxP/loxP} and lacDrd2KO mice; *n* (ad libitum) = 4 and 4 (5 mo) and 4 and 7 (10 mo); *n* (fasted) = 4 and 5 (5 mo) and 4 and 4 (10 mo) for Drd2^{loxP/loxP} and lacDrd2KO mice, respectively. *$P < 0.05$ vs. age-matched Drd2^{loxP/loxP} mice; &$P = 0.057$ vs. age-matched Drd2^{loxP/loxP} mice. *C* and *D*: pancreatic insulin concentration (μg/ng protein) in the ad libitum condition (*C*) and after an 8-h fast (*D*) in 5- and 10-mo-old female Drd2^{loxP/loxP} and lacDrd2KO mice; *n* (ad libitum) = 5 and 5 (5 mo) and 12 and 14 (10 mo), and *n* (fasted) = 6 and 6 (5 mo) and 5 and 5 (10 mo) for Drd2^{loxP/loxP} and lacDrd2KO mice, respectively; *$P < 0.0005$ vs. age-matched Drd2^{loxP/loxP} mice.
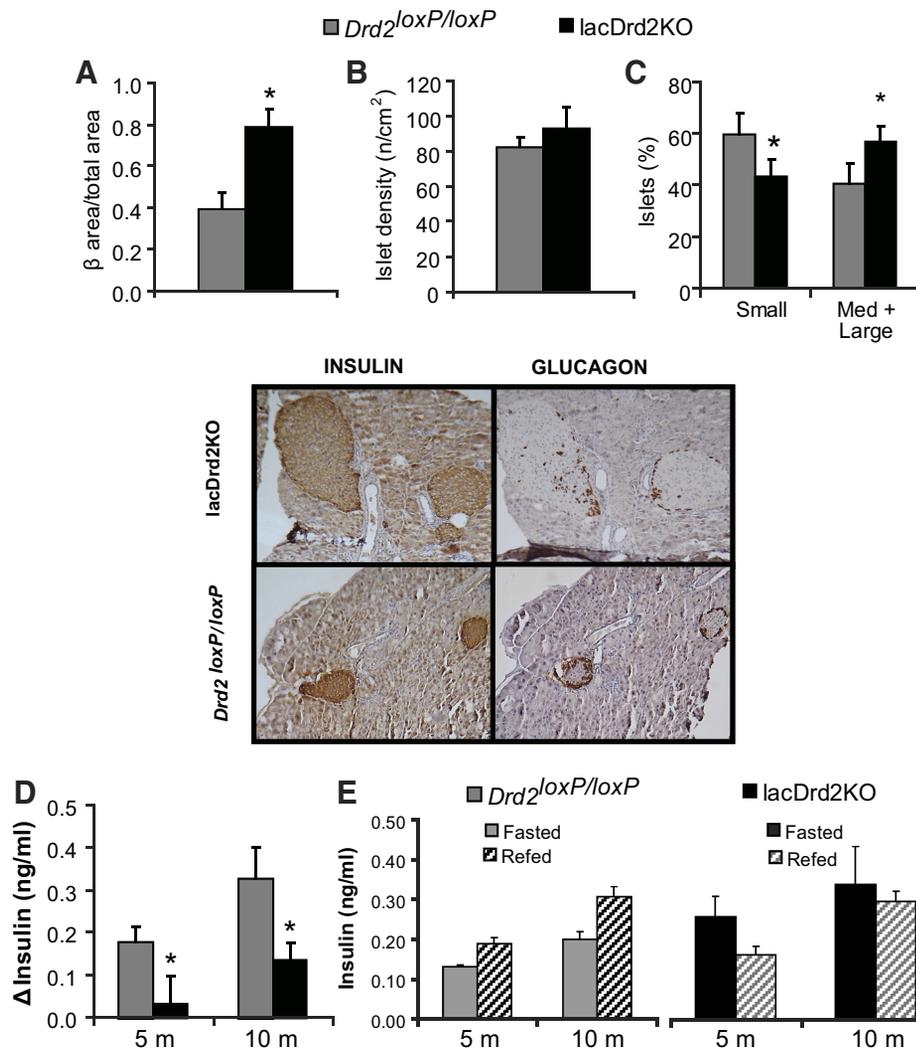
Fig. 3. Increased β-cell area and medium-large islets in pancreas from lacDrd2KO females but impaired insulin response to glucose. *A–C*: β-cell area (relative insulin-positive area/total tissue area; *A*), islet density (defined as insulin-positive aggregates of ≥20 μm diameter/cm² tissue; *B*), and percentage of small and medium-large islets (islets <5,000 μm² in size were defined as small and those >5,000 μm² as medium–large; *C*); $n = 7$ and 6 *Drd2loxP/loxP* and lacDrd2KO 5-mo-old mice, respectively. *$P< 0.05$ vs. age-matched *Drd2loxP/loxP* mice. Pictured below *A–C* are representative consecutive images of insulin (*left*) and glucagon (*right*) staining in pancreatic tissue from lacDrd2KO and *Drd2loxP/loxP* mice; specific immunolabeling is detected in brown, corresponding to the DAB dye, and cell nuclei are visualized in blue (hematoxylin counterstaining). *D*: insulin response to 3 mg/g ip glucose stimulation, expressed as Δinsulin = insulin levels after stimulation − insulin basal levels in ng/ml in 5- and 10-mo-old *Drd2loxP/loxP* and lacDrd2 female mice; $n = 6$ and 6 (5 mo) and 4 and 6 (10 mo) for *Drd2loxP/loxP* and lacDrd2KO mice, respectively. *$P< 0.02$ vs. age-matched *Drd2loxP/loxP* mice. *E*, *left*: serum insulin levels (ng/ml) in 12-h-fasted or 12-h-fasted followed by 1 h of refeeding (refed) *Drd2loxP/loxP* at 5 or 10 mo of age; $n = 4$ and 4 (5-mo-old *Drd2loxP/loxP* fasted and refed) and 4 and 5 (10-mo-old *Drd2loxP/loxP* fasted and refed); $P= 0.069$ fasted vs. refed in *Drd2loxP/loxP* mice. *E*, *right*: serum insulin levels (ng/ml) in 12-h-fasted or 12-h-fasted followed by 1 h of refeeding (refed) lacDrd2KO mice at 5 or 10 mo of age; $n = 4$ and 4 (5-mo-old lacDrd2KO fasted and refed) and 7 and 6 (10-mo-old lacDrd2KO fasted and refed).

paired at both ages in lacDrd2KO mice ($P ≤ 0.02$, lacDrd2KO vs. *Drd2loxP/loxP*; Fig. 3E). Altered insulin response was also inferred from experiments comparing genotypes after a fast-refed protocol that consisted of a 12-h fast for all animals, followed by refeeding (refed group) or fasting (fasted group) for an extra hour. Serum insulin was marginally increased in response to refeeding in 5- and 10-mo-old *Drd2loxP/loxP* mice ($P = 0.069$, for the effect of refeeding, Fig. 3E, *left*) and not in lacDrd2KO mice ($P = 0.37$; Fig. 3F, *right*).

Liver Prlr, growth hormone receptor, and glucocorticoid receptor mRNA expression. We next sought to analyze the impact of high prolactin levels and impaired insulin and glucose homeostasis on mRNA expression of liver hormone receptors. There was an increase in total (short and long isoforms) *Prlr* mRNA expression in both 5- and 10-mo-old lacDrdKO mice compared with *Drd2loxP/loxP* controls ($P = 0.029$ in 5- and $P = 0.031$ in 10-mo-old lacDrd2KO vs. age-matched *Drd2loxP/loxP* mice; Fig. 4A), which in 10-mo-old mice was driven mainly by the *Prlr-s3* isoform. Analysis of ΔC_{TS} pointed to a greater abundance of the *Prlr-s3* isoform [lower delta cycle threshold (dCT)] and an almost undetectable level of the *Prlr-s2* isoform (dCT ± SE in *Drd2loxP/loxP* mice = 6.2 ± 0.5, 6.7 ± 0.5, 11.8 ± 0.2, and 4.2 ± 0.3 for *Prlr-l, Prlr-s1, Prlr-s2,* and *Prlr-s3,* respectively).

Table 3. *Pancreas insulin and glucagon content assessed by immunohistochemistry in Drd2loxP/loxP and lacDrd2KO female mice*

	Drd2loxP/loxP	lacDrd2KO	*P* Value
Pancreas weight, g	0.298 ± 0.020	0.385 ± 0.027	0.063
Pancreas weight/BW	0.014 ± 0.001	0.015 ± 0.001	0.55
Mean islet size, μm²	7,316 ± 1,340	11,613 ± 1,582	0.081
Islets area/total area, %	0.602 ± 0.123	0.999 ± 0.104	0.048*
β-Cell fraction, %	67.21 ± 1.61	78.65 ± 2.89	0.0071*
Mean β-cell size, μm²	84.75 ± 3.16	94.88 ± 2.30	0.014*
Ratio insulin/glucagon area	2.095 ± 0.130	4.093 ± 0.517	0.0036*

Values are means ± SE. BW, body weight. *Drd2loxP/loxP*, $n = 7$; lacDrd2KO, $n = 6$. *$P < 0.05$ vs. *Drd2loxP/loxP* mice.
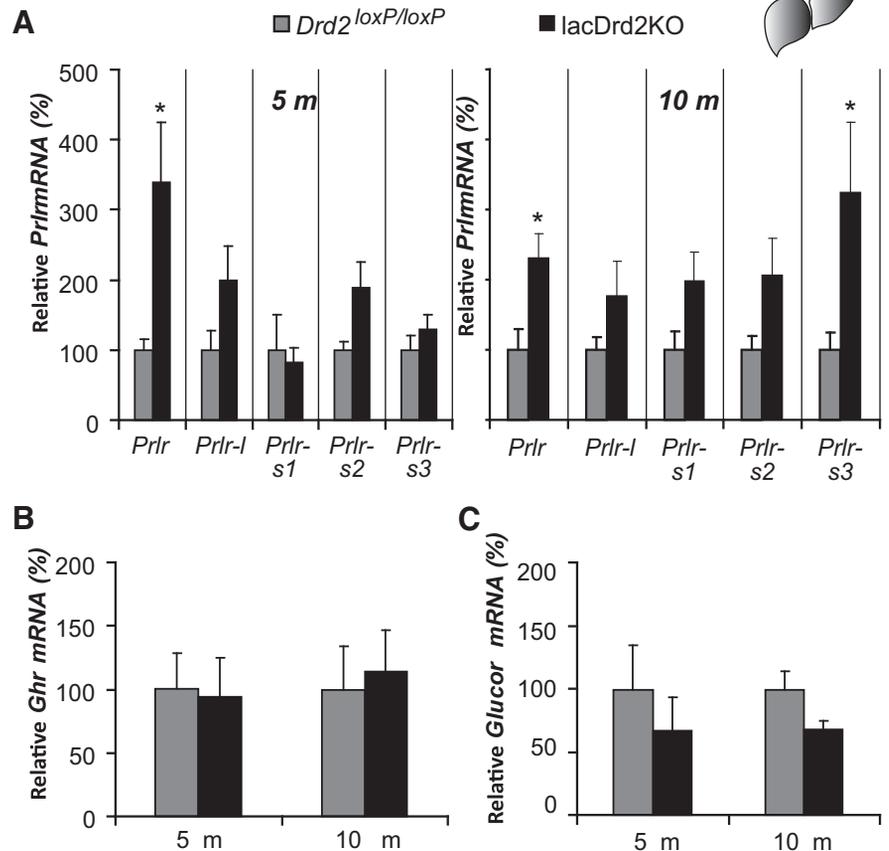
Fig. 4. Increased prolactin receptor (*Prlr*) mRNA levels in livers from lacDrd2KO females. *A*: *Prlr* mRNA levels in 5- and 10-mo-old female $Drd2^{loxP/loxP}$ and lacDrd2KO mice. *Prlr*, all isoforms; *Prlr-l*, long subtype; *Prlr-s1–3*, short isoforms 1–3; $n = 5$ and 4 (5 mo) and 6 and 7 (10 mo) $Drd2^{loxP/loxP}$ and lacDrd2KO mice, respectively. *$P < 0.05$ vs. age-matched $Drd2^{loxP/loxP}$ mice. *B*: liver *Ghr* mRNA levels; $n = 5$ and 4 (5 mo) and 7 and 7 (10 mo) $Drd2^{loxP/loxP}$ and lacDrd2KO mice, respectively. *C*: liver *Glucor* mRNA levels; $n = 5$ and 4 (5 mo) and 7 and 8 (10 mo) $Drd2^{loxP/loxP}$ and lacDrd2KO mice, respectively.

On the other hand, there were no differences between genotypes in liver growth hormone receptor (*Ghr*) or glucocorticoid receptor (*Glucor*) mRNA expression at either age (Fig. 4, *B* and *C*).

Liver Chrebp, Srebp-1c, glucokinase, and glycogen synthase mRNA expression levels and glycogen content. ChREBP and SREBP-1c are two transcription factors involved in glycolytic and lipogenic gene expression. Liver *Chrebp* mRNA expression was higher in ad libitum-fed 5-mo-old lacDrd2KO compared with $Drd2^{loxP/loxP}$ mice ($P \leq 0.03$; Fig. 5*A*), whereas no differences between genotypes were observed in 10-mo-old mice or in *Srebp-1c* expression at either age (Fig. 5*A*).

After a 12-h fast, followed by 1 h of refeeding, *Srebp-1c* mRNA expression was increased in $Drd2^{loxP/loxP}$ but not in lacDrd2KO mice (Fig. 5*C*) at 5 mo of age. This effect was not in evidence in 10-mo-old mice (Fig. 5*C*). On the other hand, liver *Chrebp* mRNA expression was not significantly modified by refeeding (Fig. 5*B*).

After glucose entry into hepatocytes, it is phosphorylated on carbon 6 by glucokinase generating glucose 6-phosphate (G6P), which may be converted into glycogen by the action of glycogen synthase (Gys) or metabolized to be used in the synthesis of fatty acids, cholesterol, and bile salts. In ad libitum-fed mice, liver glucokinase mRNA expression was increased in 10-mo-old lacDrd2KO compared with $Drd2^{loxP/loxP}$ mice ($P = 0.0015$; Fig. 6*A*), whereas no differences between genotypes were observed In *Gys* mRNA expression levels or liver glycogen concentration (Fig. 6*A*). After a 12-h fast, followed by 1 h of refeeding, glucokinase mRNA expression was increased in both genotypes and at both ages (Fig. 6*B*), the magnitude of increase being higher

in younger mice. Liver glycogen concentration also increased in response to refeeding in both genotypes and at both ages (Fig. 6*C*). These results indicate that liver de novo lipogenesis was altered, whereas the glycogen synthesis pathway was not.

Prolactin enhances Chrebp and Prlr mRNA expression in cultured hepatocytes. Hepatocytes from $Drd2^{loxP/loxP}$ 5 mo-old mice were cultured in vitro and challenged with prolactin to test a direct effect of the hormone. *Chrebp* and *Prlr* (all isoforms) mRNA expression increased after after 6, 12, and 24 h of 200 ng/ml prolactin treatment (for *Chrebp P* interaction $= 0.615$, 200 ng/ml vs. basal $P = 0.013$; for prolactin *P* interaction $= 0.397$, 200 ng/ml vs. basal $P = 0.0025$). No effect was in evidence for *Srebp-1c* or *Fas* expression (Fig. 7).

Serum cholesterol and triglyceride levels in $Drd2^{loxP/loxP}$ and lacDrd2KO mice. Serum cholesterol levels were not different between genotypes at 5 and 10 mo of age in ad libitum conditions, whereas serum triglyceride levels were increased prominently in 10-mo-old ad libitum-fed but not fasted mice (Table 4).

Normal adipose tissue Prlr, Ghr, and Glucor mRNA expression. No significant differences between genotypes were found in *Prlr*, *Ghr*, or *Glucor* mRNA expression in gonadal white adipose tissue (Fig. 8, *A–C*). In this tissue, the long isoform of the *Prlr* (*Prlr-l*) was predominant (lower dCT), whereas the *Prlr-s1* and *-s2* isoforms were barely detectable (dCT $\pm$ SE in $Drd2^{loxP/loxP}$ mice $= 4.7 \pm 0.2$; 13.8 ± 0.9; ND; and 9.4 ± 0.3 for *Prlr-l*, *Prlr-s1*, *Prlr-s2* and *Prlr-s3*, respectively).

Similar *Glucor* mRNA levels in liver and adipose tissue pointed to a conserved adrenal axis. In accordance, we found
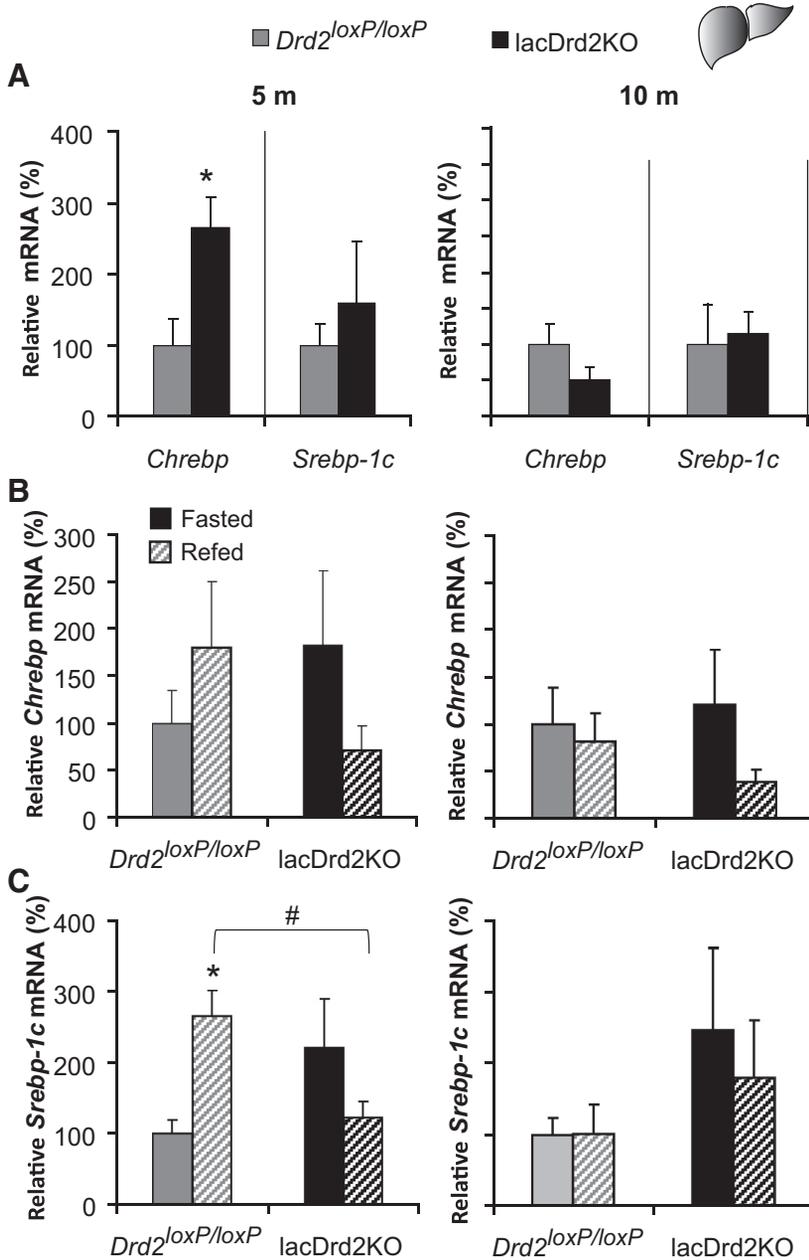
Fig. 5. Altered liver carbohydrate-responsive element-binding protein (*Chrebp*) and sterol regulatory element-binding protein-1c (*Srebp-1c*) mRNA levels in lacDrd2KO females in ad libitum fasted and refed conditions. *A*: *Chrebp* and *Srebp-1c* mRNA levels in the ad libitum condition in 5- and 10-mo-old female *Drd2^{loxP/loxP}* and lacDrd2KO mice; *n* = 5 and 4 (5 mo and 6 and 7 (10 mo) for *Drd2^{loxP/loxP}* and lacDrd2KO mice, respectively. *P < 0.05 vs. age-matched *Drd2^{loxP/loxP}* mice; for this and subsequent graphs, %target mRNA levels normalized *cyclophilin* mRNA levels in relation to age-matched *Drd2^{loxP/loxP}* mice (100%), which is represented in the *y*-axes. *B*: *Chrebp* mRNA levels in 12-h-fasted or 12-h-fasted followed by 1 h of refeeding (refed) *Drd2^{loxP/loxP}* and lacDrd2KO mice at 5 or 10 mo of age; *n* = 8 and 5 (5 mo-old *Drd2^{loxP/loxP}* fasted and refed), 8 and 8 (5-mo-old lacDrd2KO fasted and refed), 5 and 5 (10-mo-old *Drd2^{loxP/loxP}* fasted and refed), and 4 and 5 (10-mo-old lacDrd2KO fasted and refed). *C*: *Srebp-1c* mRNA levels in 12-h-fasted or 12-h-fasted followed by 1 h of refeeding (refed) *Drd2^{loxP/loxP}* and lacDrd2KO mice at 5 or 10 mo of age [*n* = 7 and 6 (5 mo-old *Drd2^{loxP/loxP}* fasted and refed), 8 and 8 (5-mo-old lacDrd2KO fasted and refed), 5 and 5 (10-mo-old *Drd2^{loxP/loxP}* fasted and refed), and 4 and 5 (10 mo-old lacDrd2KO fasted and refed]. *P < 0.05 vs. fasted *Drd2^{loxP/loxP}* mice; #P < 0.05, refed lacDrd2KO mice.

no differences between genotypes in adrenal weight or histolomorphology in 5-mo-old mice (data not shown).

Altered adipose tissue Chrebp and Srebp-1c mRNA expression levels. In 10-mo-old ad libitum, fasted and refed mice *Chrebp* was lower in lacDrd2KO compared with condition-matched *Drd2^{loxP/loxP}* mice (Fig. 9, *A* and *B*). *Srebp-1c* was also lower in the lacDrd2KO genotype in ad libitum 10-mo-old fed mice (Fig. 9*A*). Acutely refeeding mice after a fasting period induced *Chrebp* mRNA expression in both genotypes and at both ages (Fig. 9*B*), whereas *Srebp-1c* mRNA expression increased in adipose tissue from 5- but not 10-mo-old fasted mice of both genotypes (Fig. 9*C*).

DISCUSSION

Prolactin is critical during two major physiological periods, pregnancy and lactation, favoring lipid storage and glucose availability, vital requisites for meeting the energy needs of mother and offspring. Prolactin signaling orchestrates several organs to this end, including the brain, where it exerts an orexigenic action (59, 65). If prolactin is overproduced at an inappropriate time, metabolic disorders could be envisaged. For example, patients with hyperprolactinemia are prone to excessive weight gain, and normalization of prolactin levels with dopamine agonists correlates with weight loss (28, 58). There is a genetic association between prolactin and obesity, and genome wide association studies revealed a linkage of obesity to a common variant adjacent to the prolactin gene (49, 53) suggesting that abnormalities in prolactin signaling may contribute to human obesity.

Previously, we conducted a cell-specific genetic dissection study using conditional mutant mice that selectively lack D2Rs
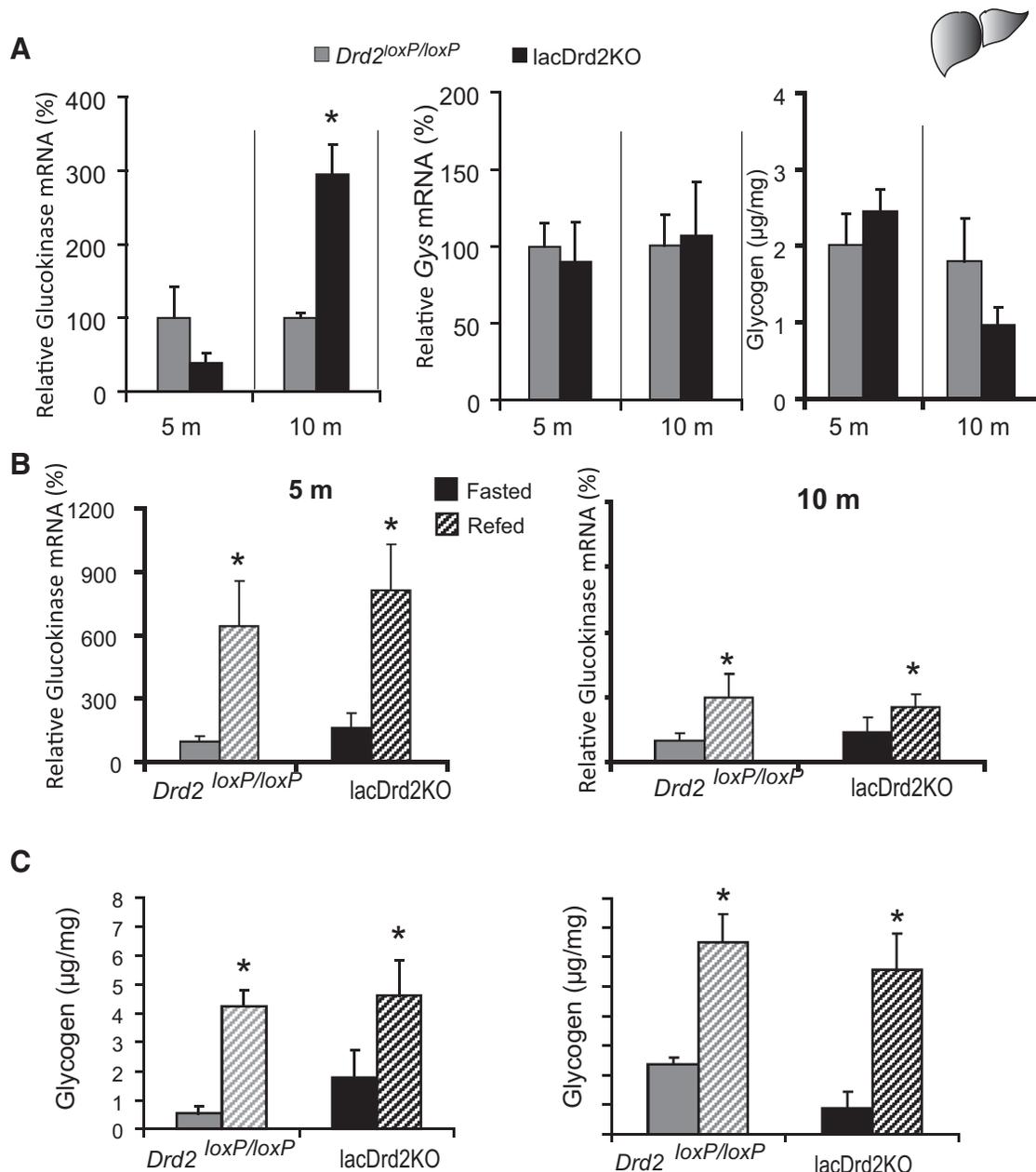
Fig. 6. Liver glucokinase and glycogen synthase (*Gys*) mRNA levels and glycogen concentration in ad libitum fasted and refed conditions. *A*: flucokinase and *Gys* mRNA levels and glycogen content (μg/mg) in the ad libitum condition in 5- and 10-mo-old female *Drd2^{loxP/loxP}* and lacDrd2KO mice; *n* = 5 and 4 (5 mo) and 6 and 7 (10 mo) for *Drd2^{loxP/loxP}* and lacDrd2KO mice, respectively, and 5 and 5 (5 mo) and 9 and 7 (10 mo) for glycogen concentration for *Drd2^{loxP/loxP}* and lacDrd2KO mice, respectively. *$P < 0.01$ vs. age-matched *Drd2^{loxP/loxP}* mice. *B*: glucokinase mRNA levels in 12-h-fasted or 12-h-fasted followed by 1 h of refeeding (refed) *Drd2^{loxP/loxP}* and lacDrd2KO mice at 5 or 10 mo of age; *n* = 7 and 6 (5-mo-old *Drd2^{loxP/loxP}* fasted and refed), 8 and 8 (5-mo-old lacDrd2KO fasted and refed), 5 and 4 (10-mo-old *Drd2^{loxP/loxP}* fasted and refed), and 5 and 5 (10-mo-old lacDrd2KO fasted and refed). In *A* and *B*, %target mRNA levels normalized *cyclophilin* mRNA levels in relation to age-matched fasted *Drd2^{loxP/loxP}* mice (100%), which is represented in the *y*-axis. *C*: glycogen content in 12-h-fasted or 12-h-fasted followed by 1 h of refeeding (refed) *Drd2^{loxP/loxP}* and lacDrd2KO mice at 5 or 10 mo of age; *n* = 6 and 4 (5-mo-old *Drd2^{loxP/loxP}* fasted and refed), 5 and 4 (5-mo-old lacDrd2KO fasted and refed), 5 and 4 (10-mo-old *Drd2^{loxP/loxP}* fasted and refed), and 5 and 5 (10-mo-old lacDrd2KO fasted and refed). *$P < 0.05$ vs. fasted *Drd2^{loxP/loxP}* mice; #$P < 0.05$ refed lacDrd2KO mice.

from pituitary lactotropes (lacDrd2KO) to evaluate the role of elevated prolactin levels on metabolism and demonstrated that 11-mo-old lacDrd2KO female mice have increased body weight, fatty liver, and adiposity accretion (59). High lipid content in the liver correlated with increased triglyceride content and liver weight, but no alterations in the lipolytic (adipose triglyceride lipase and hormone-sensitive lipase) or lipogenic (fatty acid synthase and lipoprotein lipase) enzymes were

found, indicating that other mechanisms may be involved in increased lipid content in the liver. On the other hand, gross adiposity correlated with marked increments in fat depots, adipocyte size, serum triglycerides, and nonesterified fatty acid levels. In adipose tissue, decreased expression of lipolytic enzymes (adipose triglyceride lipase and hormone-sensitive lipase) could explain increased lipid droplets, but there was no evidence of increased lipogenic enzymes. In the present study,
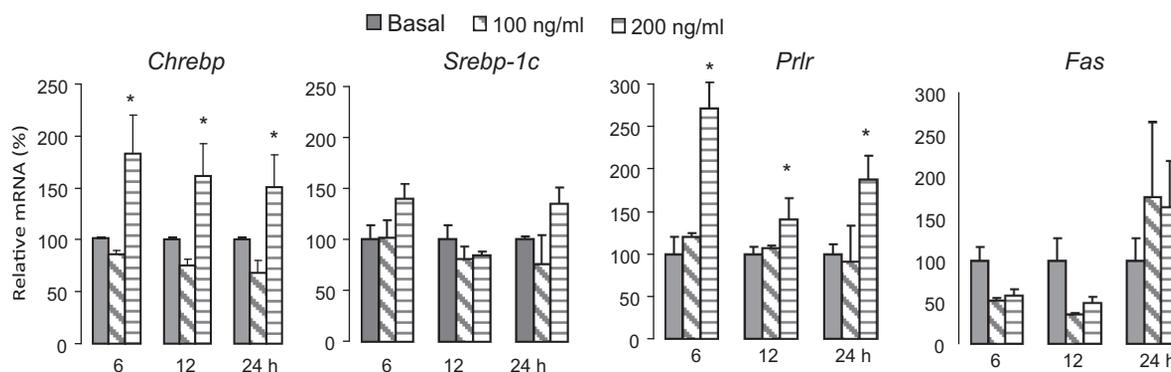
Fig. 7. Prolactin enhances *Chrebp* and *Prlr* mRNA expression in cultured hepatocytes. Effect of prolactin (0, 100, or 200 ng/ml) on *Chrebp*, *Srebp-1c*, *Prlr*, and *Fas* mRNA levels after 6, 12, or 24 h of incubation. Results are expressed as %expression of target genes normalized to *cyclophilin* mRNA levels to expression in cells incubated without prolactin (basal) at the same time points, which was considered 100%. *$P < 0.05$ vs. basal incubated cells; $n = 3$ cell cultures, replicate measures in each culture.

we aimed to establish the role of hyperprolactinemia on the expression of transcription factors and enzymes involved in lipogenesis in the liver and adipose tissue during the development of obesity in the mutant model.

Prolactin receptors exist in various isoforms, short and long, depending on the length of the cytoplasmic domain (12, 51). They are widely distributed in tissues, and hence, if prolactin levels increase supraphysiologically, there is a potential risk for a wide variety of systems to be influenced. We found increased liver *Prlr* mRNA levels in lacDrd2KO, with predominance of the s3 short isoform; furthermore, a direct effect of prolactin on liver gene expression could be inferred from in vitro experiments. In this regard, it has been demonstrated that prolactin may upregulate its cognate receptor in epididymal adipocytes (8) and breast cancer cells (40). On the other hand, in adipose tissue there was a predominance of the long isoform of the *Prlr* mRNA, and no significant modification of *Prlr* mRNA levels was observed between genotypes. In this respect, it has been documented that adipocyte responsiveness to prolactin is moderate compared with the strong responsiveness to GH (18, 42).

Although marked obesity was not evident in 5-mo-old mice, glucose intolerance and hyperinsulinemia were already present at this age, as described previously in 7-mo-old mice (59), and our present results indicate that both glucose intolerance and hypersinulinemia persisted throughout life. Glucose intolerance at 5 mo could not be explained by increased body weight but may be related to the impaired response of insulin secretion to glucose overload found in lacDrd2KO mice. Furthermore, the increased insulin and decreased glucagon pancreatic content described favor a role for prolactin at the pancreas and is consistent with the fact that prolactin promotes islet growth and function (9, 23). These actions are of paramount importance in

the adaptive metabolic response during pregnancy (35) and should be tightly regulated to prevent gestational diabetes.

Long-term exposure of the liver to elevated glucose and insulin levels modifies transcription and translation of key enzymes involved in lipogenesis. SREBP-1c and ChREBP are transcription factors of the basic helix-loop-helix leucine zipper family (34, 78) that are involved in fatty acid, glucose, and cholesterol metabolism (16) and that are differentially regulated by insulin and glucose (16, 39).

In the liver, SREBP-1c and its lipogenic target genes are transcriptionally stimulated by insulin (21) and repressed by glucagon (22). ChREBP is abundantly expressed in liver and white and brown adipose tissues (38), active sites of de novo lipogenesis, and together with SREBP-1c is a crucial modulator of transcriptional control of lipogenic genes (16). Hepatic *Chrebp* expression in induced mainly by glucose and high carbohydrate diet. During fasting, the actions of the both lipogenic transcription factors ChREBP and SREBP-1c are suppressed, and refeeding produces hyperglycemia and insulin release, which cause activation of ChREBP (38) and SREBP-1c, respectively, to initiate lipogenesis (72).

A relation of prolactin or PRLRs with liver or adipocyte *Srebp-1c* and *Chrebp* expression has not been explored. It has been reported that *Prlr*-deficient mice were highly resistant to high-fat diet-induced obesity with improved glucose homeostasis, insulin resistance, and conservation of insulin secretion (3). These *Prlr*-disrupted mice had lower *Srebp-1c* in prerenal and not subcutaneous white adipose tissue (3) in standard fed conditions, suggesting an effect of prolactin on *Srebp-1c* expression in adipose tissue, whereas the effect on the liver was not studied.

Our results point to tissue- and age-specific alteration in liver *Srebp-1c* and *Chrebp* expression in hyperprolactinemic mice. Refeeding mice after an overnight fast induced

Table 4. *Serum cholesterol and triglyceride levels in Drd2^loxP/loxP^ and lacDrd2KO female mice*

	5 Mo			10 Mo		
	*Drd2^loxP/loxP^*	lacDrd2KO	P Value	*Drd2^loxP/loxP^*	lacDrd2KO	P Value
Serum cholesterol (ad libitum)	59.0 ± 15.7	61.3 ± 18.9	0.93	62.0 ± 10.9	71.3 ± 10.0	0.58
Serum triglycerides (fasted)	104.0 ± 17.6	88.0 ± 16.9	0.57	99.0 ± 16.3	80.0 ± 20.1	0.53
Serum triglycerides (ad libitum)	125.0 ± 13.0	95.7 ± 8.8	0.11	141.3 ± 13.0	248.0 ± 40.8	0.046*

Values are means ± SE; $n = 5–7$ for each group. *$P < 0.05$ vs. condition-matched *Drd2^loxP/loxP^* mice.
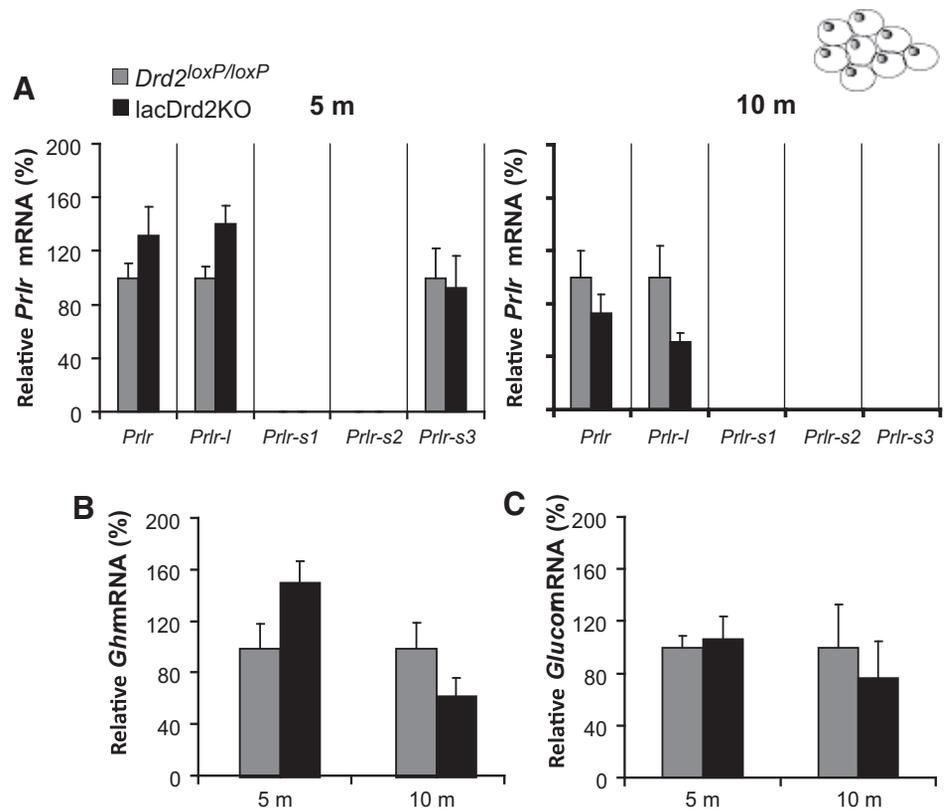
Fig. 8. Adipose tissue *Prlr*, *Ghr*, and *Glucor* mRNA levels are not modified. *A*: *Prlr* mRNA levels in 5- and 10-mo-old *Drd2*$^{loxP/loxP}$ and lacDrd2KO female mice. *Prlr*, all isoforms; *Prlr-l*, long subtype; *Prlr-s1–3*, short isoforms 1–3; *n* = 5 and 5 (5 mo) and 11 and 11 (10 mo) *Drd2*$^{loxP/loxP}$ and lacDrd2KO mice, respectively; for this and subsequent graphs, %target mRNA levels normalized *cyclophilin* mRNA levels in relation to age-matched *Drd2*$^{loxP/loxP}$ mice (100%), which is represented in the *y*-axes. *B*: adipose tissue *Ghr* mRNA levels; *n* = 5 and 4 (5 mo) and 11 and 11 (10 mo) *Drd2*$^{loxP/loxP}$ and lacDrd2KO mice, respectively. *C*: adipose tissue *Glucor* mRNA levels; *n* = 5 and 4 (5 mo) and 11 and 11 (10 mo) *Drd2*$^{loxP/loxP}$ and lacDrd2KO mice, respectively.

Srebp-1c mRNA expression in the liver of 5-mo-old *Drd2*$^{loxP/loxP}$ mice, but there was marked loss of response in age-matched lacDrd2KO mice and a desensitization of the effect in older mice. Refeeding induces de novo lipogenesis, which is associated with *Srebp-1c* expression (34), and *Srebp-1c* is regulated by insulin. As pointed out above, the insulin response to refeeding or to glucose administration was impaired in lacDrd2KO mice. Therefore, failure of liver *Srebp-1c* gene induction in hyperprolactinemic mice may be associated with inappropriate insulin release by refeeding or an early desensitization of the response and identifies an alteration of de novo lipogenesis pathways in liver already at 5 mo of age, when obesity is not fully settled. We could not detect a direct role of prolactin on hepatocyte *Srebp-1c* mRNA levels, also pointing to insulin as the cause of the inadequate response.

On the other hand, before morbid adiposity onset (i.e., at 5 mo), liver *Chrebp* mRNA expression was increased in lacDrd2KO mice in the ad libitum condition compared with *Drd2*$^{loxP/loxP}$ mice. Increased liver *Chrebp* at this age may result from a direct effect of prolactin, as we demonstrate in vitro, but we cannot rule out the participation of high glucose or insulin levels found in our experimental model (39). Increased *Chrebp* indicates de novo lipogenesis in correlation with increased liver weight in this genotype already at this age (59). The lack of liver *Chrebp* increase in lacDrd2KO mice at 10 mo of age may indicate an adaptive response aimed at limiting further expansion of fat storage and suggests that lipogenesis is a dynamic process that varies according to the development of obesity. On the other hand, liver *Chrebp* mRNA levels were not significantly modified by refeeding in either genotype, consistent with data that suggest that *Chrebp*

mRNA levels in liver and adipose tissue in vivo are barely responsive to changes in nutrient status (43). On the other hand, in contradiction to published data (43), our results point to a striking tissue-specific response of *Chrebp* to refeeding, as in adipose tissue and not in liver a consistent upregulation was observed. Furthermore, our results suggest that acute *Chrebp* response to refeeding after prolonged fasting is not comparable with an ad libitum condition, in which continuous high prolactin, insulin, and glucose levels maintained high liver *Chrebp* expression at 5 mo.

Although higher levels of liver glucokinase were observed in ad libitum lacDrd2KO mice at 10 mo of age, *Gys* mRNA levels and glycogen content were not altered significantly. The tendency observed for lower glycogen in 10-mo-old obese animals might be the result of increased lipid content per milligram of tissue. Furthermore, similar glucokinas, and glycogen responses to refeeding were obtained in both genotypes. One-hour refeeding did not increase glucokinase levels to those in ad libitum-fed lacDrd2KO mice at 5 mo of age.

Therefore, the results obtained in liver tissue suggest that the lipogenic signaling pathway was altered during chronic hyperprolactinemia, whereas no marked evidence of alterations in the glycogenic pathway was found.

On the other hand, the role of SREBP-1c and ChREBP on lipogenesis in adipose tissue has not been conclusively settled (75). White adipose tissue was not significantly decreased in *Srebp-1c*-disrupted mice (67), and double *Srebpc-1c* and *ob/ob* knockout mice showed that *Srebp-1*c was not determinant in obesity outcome, although improved fatty livers were in evidence in the double knockout (77). *Chrebp* is expressed in rat and human adipose tissue (44) and activated during differentiation of preadipocytes to adipocytes (37), suggesting its
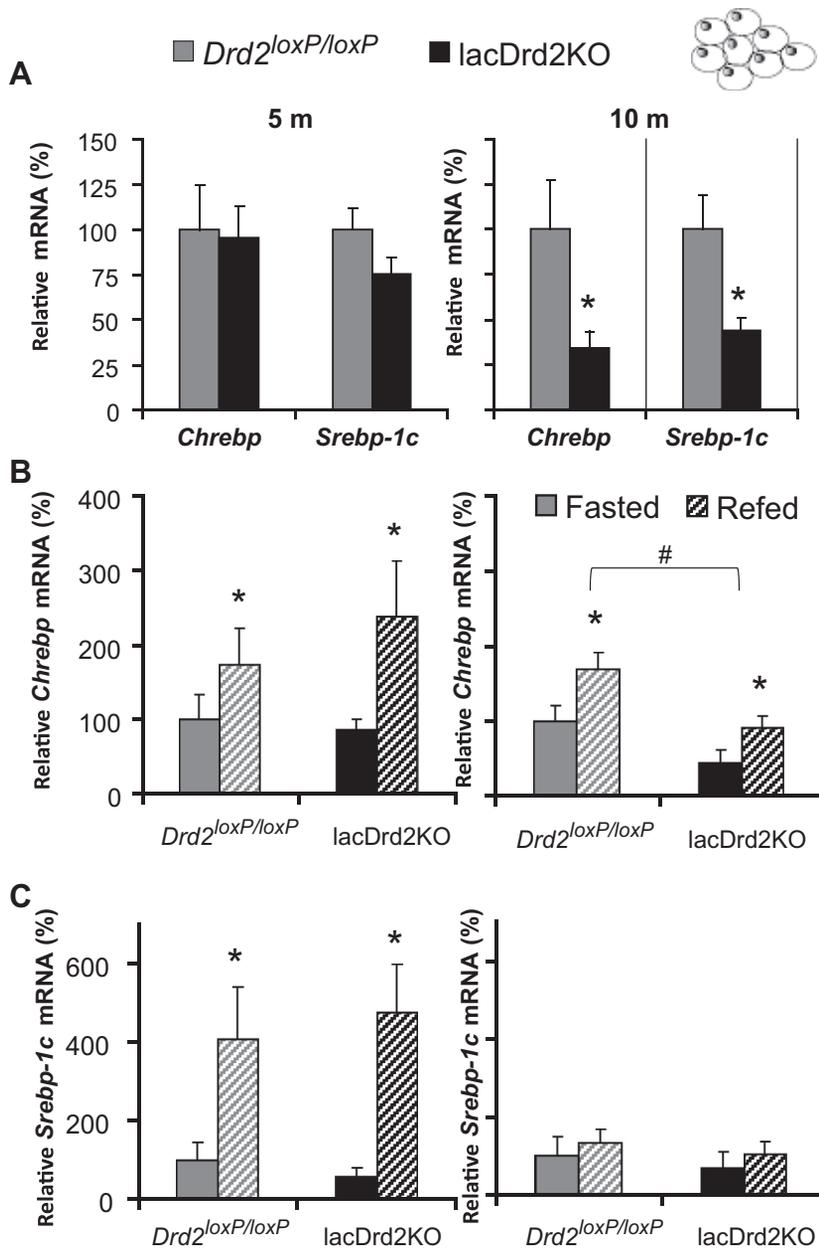
Fig. 9. Adipose tissue *Chrebp* and *Srebp-1c* mRNA levels in ad libitum fasted and refed conditions. *A*: *Chrebp* and *Srebp-1c* mRNA levels in the ad libitum condition in 5- and 10-mo-old female *Drd2$^{loxP/loxP}$* and lacDrd2KO mice; $n = 5$ and 4 (5 mo) and 10 and 9 (10 mo) for *Drd2$^{loxP/loxP}$* and lacDrd2KO mice, respectively. *$P < 0.05$ vs. age-matched *Drd2$^{loxP/loxP}$* mice; for this and subsequent graphs, %target mRNA levels normalized *cyclophilin* mRNA levels in relation to age-matched fasted *Drd2$^{loxP/loxP}$* mice (100%), which is represented in the *y*-axes. *B*: *Chrebp* mRNA levels in 12-h-fasted or 12-h-fasted followed by 1 h of refeeding (refed) *Drd2$^{loxP/loxP}$* and lacDrd2KO mice at 5 or 10 mo of age; $n = 8$ and 6 (5-mo-old *Drd2$^{loxP/loxP}$* fasted and refed), 8 and 8 (5-mo-old lacDrd2KO fasted and refed), 5 and 4 (10-mo-old *Drd2$^{loxP/loxP}$* fasted and refed), and 4 and 4 (10-mo-old lacDrd2KO fasted and refed). *$P < 0.05$ vs. genotype and age-matched fasted mice; #$P < 0.05$, condition-matched mice (lacDrd2KO vs. *Drd2$^{loxP/loxP}$*). *C*: *Srebp-1c* mRNA levels in 12-h-fasted or 12-h-fasted followed by 1 h of refeeding (refed) *Drd2$^{loxP/loxP}$* and lacDrd2KO mice at 5 or 10 mo of age; $n = 6$ and 4 (5-mo-old *Drd2$^{loxP/loxP}$* fasted and refed), 6 and 6 (5-mo-old lacDrd2KO fasted and refed), 5 and 4 (10-mo-old *Drd2$^{loxP/loxP}$* fasted and refed), and 4 and 4 (10-mo-old lacDrd2KO fasted and refed). *$P < 0.05$ vs. fasted *Drd2$^{loxP/loxP}$* mice.

participation in adipocyte adipogenesis. Nevertheless, the physiological role of ChREBP and SREBP-1c in adipose tissue warrants clarification.

In the present work, *Srebp-1c* and *Chrebp* mRNA expression levels were markedly altered in adipocytes from lacDrd2KO mice. In the ad libitum condition, *Srebp-1c* mRNA expression was lower in 10- but not in 5-mo-old lacDrd2KO mice. These results resemble *Srebp-1c* decrease in adipose tissue observed in a model of induced obesity (77) and in adipocytes of patients with morbid obesity (11), indicating that the decrease in adipose tissue *Srebp-1c* expression observed in lacDrd2KO mice may be associated with the adiposity accretion at this age. Furthermore, it has been suggested that increased leptin levels may downregulate *Srebp-1c* expression (56). Nevertheless, adipocyte *Srebp-1c* expression was induced by feeding at 5 mo of age in both genotypes, denoting a preserved response to a feeding stimulus. Present results point

to tissue specific regulation of *Srebp-1c* and suggest that its expression in adipocytes may be less dependent on insulin levels compared with hepatocytes. Furthermore, adipose tissue *Chrebp* expression was decreased in obese 10-mo-old mice not only in the ad libitum condition but also in fasted and refed conditions. It has been demonstrated that genetically altering adipose tissue glucose flux regulates the expression of ChREBP and its lipogenic targets (32). Nevertheless, *Chrebp* mRNA levels in response to refeeding were similar between genotypes. These data indicate a preserved induction of this transcription factor to refeeding but a tissue- and age-specific alteration of *Chrebp*. A similar decrease has been found in adipose tissue from obese subjects (36) and in high-fat diet-fed mice (32).

Contrary to the initial expectations, in obese mice due to leptin deficiency, adipocyte expression of numerous genes involved in cell differentiation and adipogenesis, including

SREBP, was actually downregulated, suggesting a process of loss of adipocyte phenotype or desensitization of nutrient sensors with advancing obesity (50). In the early stages of adipocyte differentiation in vitro and in vivo, many of these genes are upregulated (69) indicating ongoing adipocyte hypertrophy and fat accumulation, and at later stages expression markedly decreases, as in our present mouse model. The finding that obesity leads to a downregulation of markers that characterize mature, metabolically active adipose cells suggests that adipocytes from obese mice and humans have a decreased lipogenic capacity and underscore the complex process of lipid accumulation in which gene expression profiles in adipocytes vary according to the different stages of development of obesity (1).

Prolactin receptors have been found in the adrenal gland, and in particular prolactin activates STAT phosphorylation in the adrenal cortex and not in the medulla (42). Nevertheless, we did not find differences in adrenal weight, or *Glucor* in adipose tissue and liver in lacDrd2KO compared with *Drd2^{loxP/loxP}* mice, which is indicative of the absence of altered secretion of glucocorticoids.

In conclusion, we propose that chronic hyperprolactinemia upregulates liver *Prlr* and evokes liver steatosis, enhancement of the lipogenic transcription factor *Chrebp*, and alteration in the *Srebp-1c* response to refeeding; whereas in adipose tissue marked adiposity is associated with a decrease in both transcription factors. These adaptive changes may be linked with glucose intolerance, hyperinsulinemia, and impaired insulin response to glucose, which are already evident in early stages of obesity, whereas a direct effect of prolactin on hepatocyte function cannot be ruled out, and underscore the role of prolactin signaling in different tissues to promote energy storage. In humans, hyperprolactinemia may be associated with hyperinsulinemia and insulin resistance (66, 79), and accumulation of toxic lipids is the most common etiology of insulin resistance in type 2 diabetes and associated metabolic disorders such as obesity and nonalcoholic fatty liver disease. Therefore, understanding of the underlying mechanisms of metabolic manifestations during untimely prolactin overproduction may reveal opportunities to target key regulators in lipid metabolic pathways for the treatment of metabolic diseases.

DISCLOSURES

No conflicts of interest, financial or otherwise, are declared by the authors.

AUTHOR CONTRIBUTIONS

G.M.L., F.L.-V., A.M.O., B.B., C.D.W., E.F., M.I.P.M., G.M., and D.B.-V. performed experiments; G.M.L., F.L.-V., and D.B.-V. analyzed data; G.M.L., M.R., and D.B.-V. interpreted results of experiments; G.M.L. and D.B.-V. prepared figures; G.M.L., F.L.-V., M.R., and D.B.-V. edited and revised manuscript; G.M.L., F.L.-V., A.M.O., B.B., C.D.W., M.I.P.M., M.R., and D.B.-V. approved final version of manuscript; D.B.-V. drafted manuscript.

REFERENCES

1. **Al-Hasani H, Joost HG.** Nutrition-/diet-induced changes in gene expression in white adipose tissue. *Best Pract Res Clin Endocrinol Metab* 19: 589–603, 2005. doi:10.1016/j.beem.2005.07.005.

2. **Asai-Sato M, Okamoto M, Endo M, Yoshida H, Murase M, Ikeda M, Sakakibara H, Takahashi T, Hirahara F.** Hypoadiponectinemia in lean lactating women: Prolactin inhibits adiponectin secretion from human adipocytes. *Endocr J* 53: 555–562, 2006. doi:10.1507/endocrj.K06-026.

3. **Auffret J, Viengchareun S, Carré N, Denis RG, Magnan C, Marie PY, Muscat A, Fève B, Lombès M, Binart N.** Beige differentiation of adipose depots in mice lacking prolactin receptor protects against high-fat-diet-induced obesity. *FASEB J* 26: 3728–3737, 2012. doi:10.1096/fj.12-204958.

4. **Bacon RL, Kirkman H.** The response of the testis of the hamster to chronic treatment with different estrogens. *Endocrinology* 57: 255–271, 1955. doi:10.1210/endo-57-3-255.

5. **Bello EP, Mateo Y, Gelman DM, Noaín D, Shin JH, Low MJ, Alvarez VA, Lovinger DM, Rubinstein M.** Cocaine supersensitivity and enhanced motivation for reward in mice lacking dopamine D2 autoreceptors. *Nat Neurosci* 14: 1033–1038, 2011. doi:10.1038/nn.2862.

6. **Benhamed F, Denechaud PD, Lemoine M, Robichon C, Moldes M, Bertrand-Michel J, Ratziu V, Serfaty L, Housset C, Capeau J, Girard J, Guillou H, Postic C.** The lipogenic transcription factor ChREBP dissociates hepatic steatosis from insulin resistance in mice and humans. *J Clin Invest* 122: 2176–2194, 2012. doi:10.1172/JCI41636.

7. **Bole-Feysot C, Goffin V, Edery M, Binart N, Kelly PA.** Prolactin (PRL) and its receptor: actions, signal transduction pathways and phenotypes observed in PRL receptor knockout mice. *Endocr Rev* 19: 225–268, 1998. doi:10.1210/edrv.19.3.0334.

8. **Brandebourg TD, Bown JL, Ben-Jonathan N.** Prolactin upregulates its receptors and inhibits lipolysis and leptin release in male rat adipose tissue. *Biochem Biophys Res Commun* 357: 408–413, 2007. doi:10.1016/j.bbrc.2007.03.168.

9. **Brelje TC, Stout LE, Bhagroo NV, Sorenson RL.** Distinctive roles for prolactin and growth hormone in the activation of signal transducer and activator of transcription 5 in pancreatic islets of langerhans. *Endocrinology* 145: 4162–4175, 2004. doi:10.1210/en.2004-0201.

10. **Buck K, Vanek M, Groner B, Ball RK.** Multiple forms of prolactin receptor messenger ribonucleic acid are specifically expressed and regulated in murine tissues and the mammary cell line HC11. *Endocrinology* 130: 1108–1114, 1992.

11. **Carobbio S, Hagen RM, Lelliott CJ, Slawik M, Medina-Gomez G, Tan CY, Sicard A, Atherton HJ, Barbarroja N, Bjursell M, Bohlooly-Y M, Virtue S, Tuthill A, Lefai E, Laville M, Wu T, Considine RV, Vidal H, Langin D, Oresic M, Tinahones FJ, Fernandez-Real JM, Griffin JL, Sethi JK, López M, Vidal-Puig A.** Adaptive changes of the Insig1/SREBP1/SCD1 set point help adipose tissue to cope with increased storage demands of obesity. *Diabetes* 62: 3697–3708, 2013. doi:10.2337/db12-1748.

12. **Clarke DL, Linzer DI.** Changes in prolactin receptor expression during pregnancy in the mouse ovary. *Endocrinology* 133: 224–232, 1993.

13. **Davis JA, Linzer DI.** Expression of multiple forms of the prolactin receptor in mouse liver. *Mol Endocrinol* 3: 674–680, 1989. doi:10.1210/mend-3-4-674.

14. **Dentin R, Pégorier JP, Benhamed F, Foufelle F, Ferré P, Fauveau V, Magnuson MA, Girard J, Postic C.** Hepatic glucokinase is required for the synergistic action of ChREBP and SREBP-1c on glycolytic and lipogenic gene expression. *J Biol Chem* 279: 20314–20326, 2004. doi:10.1074/jbc.M312475200.

15. **Dimitriadis G, Mitrou P, Lambadiari V, Maratou E, Raptis SA.** Insulin effects in muscle and adipose tissue. *Diabetes Res Clin Pract* 93, *Suppl* 1: S52–S59, 2011. doi:10.1016/S0168-8227(11)70014-6.

16. **Filhoulaud G, Guilmeau S, Dentin R, Girard J, Postic C.** Novel insights into ChREBP regulation and function. *Trends Endocrinol Metab* 24: 257–268, 2013. doi:10.1016/j.tem.2013.01.003.

17. **Fiore EJ, Bayo JM, Garcia MG, Malvicini M, Lloyd R, Piccioni F, Rizzo M, Peixoto E, Sola MB, Atorrasagasti C, Alaniz L, Camilletti MA, Enguita M, Prieto J, Aquino JB, Mazzolini G.** Mesenchymal stromal cells engineered to produce IGF-I by recombinant adenovirus ameliorate liver fibrosis in mice. *Stem Cells Dev* 24: 791–801, 2015. doi:10.1089/scd.2014.0174.

18. **Fleenor D, Arumugam R, Freemark M.** Growth hormone and prolactin receptors in adipogenesis: STAT-5 activation, suppressors of cytokine signaling, and regulation of insulin-like growth factor I. *Horm Res* 66: 101–110, 2006. doi:10.1159/000093667.

19. **Flint DJ, Binart N, Boumard S, Kopchick JJ, Kelly P.** Developmental aspects of adipose tissue in GH receptor and prolactin receptor gene disrupted mice: site-specific effects upon proliferation, differentiation and hormone sensitivity. *J Endocrinol* 191: 101–111, 2006. doi:10.1677/joe.1.06939.

20. **Flint DJ, Binart N, Kopchick J, Kelly P.** Effects of growth hormone and prolactin on adipose tissue development and function. *Pituitary* 6: 97–102, 2003. doi:10.1023/B:PITU.0000004800.57449.67.

21. **Foretz M, Guichard C, Ferré P, Foufelle F.** Sterol regulatory element binding protein-1c is a major mediator of insulin action on the hepatic expression of glucokinase and lipogenesis-related genes. *Proc Natl Acad Sci USA* 96: 12737–12742, 1999. doi:10.1073/pnas.96.22.12737.

22. **Foretz M, Pacot C, Dugail I, Lemarchand P, Guichard C, Le Lièpvre X, Berthelier-Lubrano C, Spiegelman B, Kim JB, Ferré P, Foufelle F.** ADD1/SREBP-1c is required in the activation of hepatic lipogenic gene expression by glucose. *Mol Cell Biol* 19: 3760–3768, 1999. doi:10.1128/MCB.19.5.3760.

23. **Freemark M, Avril I, Fleenor D, Driscoll P, Petro A, Opara E, Kendall W, Oden J, Bridges S, Binart N, Breant B, Kelly PA.** Targeted deletion of the PRL receptor: effects on islet development, insulin production, and glucose tolerance. *Endocrinology* 143: 1378–1385, 2002. doi:10.1210/endo.143.4.8722.

24. **Galsgaard ED, Nielsen JH, Møldrup A.** Regulation of prolactin receptor (PRLR) gene expression in insulin-producing cells. Prolactin and growth hormone activate one of the rat prlr gene promoters via STAT5a and STAT5b. *J Biol Chem* 274: 18686–18692, 1999. doi:10.1074/jbc.274.26.18686.

25. **García-Tornadú I, Díaz-Torga G, Risso GS, Silveyra P, Cataldi N, Ramirez MC, Low MJ, Libertun C, Becu-Villalobos D.** Hypothalamic orexin, OX1, alphaMSH, NPY and MCRs expression in dopaminergic D2R knockout mice. *Neuropeptides* 43: 267–274, 2009. doi:10.1016/j.npep.2009.06.002.

26. **García-Tornadú I, Ornstein AM, Chamson-Reig A, Wheeler MB, Hill DJ, Arany E, Rubinstein M, Becu-Villalobos D.** Disruption of the dopamine d2 receptor impairs insulin secretion and causes glucose intolerance. *Endocrinology* 151: 1441–1450, 2010. doi:10.1210/en.2009-0996.

27. **Grattan DR.** 60 YEARS OF NEUROENDOCRINOLOGY: The hypothalamo-prolactin axis. *J Endocrinol* 226: T101–T122, 2015. doi:10.1530/JOE-15-0213.

28. **Greenman Y, Tordjman K, Stern N.** Increased body weight associated with prolactin secreting pituitary adenomas: weight loss with normalization of prolactin levels. *Clin Endocrinol (Oxf)* 48: 547–553, 1998. doi:10.1046/j.1365-2265.1998.00403.x.

29. **Gualillo O, Lago F, García M, Menéndez C, Señarís R, Casanueva FF, Diéguez C.** Prolactin stimulates leptin secretion by rat white adipose tissue. *Endocrinology* 140: 5149–5153, 1999.

30. **Hagiwara A, Cornu M, Cybulski N, Polak P, Betz C, Trapani F, Terracciano L, Heim MH, Rüegg MA, Hall MN.** Hepatic mTORC2 activates glycolysis and lipogenesis through Akt, glucokinase, and SREBP1c. *Cell Metab* 15: 725–738, 2012. doi:10.1016/j.cmet.2012.03.015.

31. **Hartwell HJ, Petrosky KY, Fox JG, Horseman ND, Rogers AB.** Prolactin prevents hepatocellular carcinoma by restricting innate immune activation of c-Myc in mice. *Proc Natl Acad Sci USA* 111: 11455–11460, 2014. doi:10.1073/pnas.1404267111.

32. **Herman MA, Peroni OD, Villoria J, Schön MR, Abumrad NA, Blüher M, Klein S, Kahn BB.** A novel ChREBP isoform in adipose tissue regulates systemic glucose metabolism. *Nature* 484: 333–338, 2012. doi:10.1038/nature10986.

33. **Horseman ND, Gregerson KA.** Prolactin actions. *J Mol Endocrinol* 52: R95–R106, 2013. doi:10.1530/JME-13-0220.

34. **Horton JD, Bashmakov Y, Shimomura I, Shimano H.** Regulation of sterol regulatory element binding proteins in livers of fasted and refed mice. *Proc Natl Acad Sci USA* 95: 5987–5992, 1998. doi:10.1073/pnas.95.11.5987.

35. **Huang C, Snider F, Cross JC.** Prolactin receptor is required for normal glucose homeostasis and modulation of beta-cell mass during pregnancy. *Endocrinology* 150: 1618–1626, 2009. doi:10.1210/en.2008-1003.

36. **Hurtado del Pozo C, Vesperinas-García G, Rubio MÁ, Corripio-Sánchez R, Torres-García AJ, Obregon MJ, Calvo RM.** ChREBP expression in the liver, adipose tissue and differentiated preadipocytes in human obesity. *Biochim Biophys Acta* 1811: 1194–1200, 2011. doi:10.1016/j.bbalip.2011.07.016.

37. **Iizuka K.** Recent progress on the role of ChREBP in glucose and lipid metabolism. *Endocr J* 60: 543–555, 2013. doi:10.1507/endocrj.EJ13-0121.

38. **Iizuka K, Bruick RK, Liang G, Horton JD, Uyeda K.** Deficiency of carbohydrate response element-binding protein (ChREBP) reduces lipogenesis as well as glycolysis. *Proc Natl Acad Sci USA* 101: 7281–7286, 2004. doi:10.1073/pnas.0401516101.

39. **Iizuka K, Horikawa Y.** ChREBP: a glucose-activated transcription factor involved in the development of metabolic syndrome. *Endocr J* 55: 617–624, 2008. doi:10.1507/endocrj.K07E-110.

40. **Kavarthapu R, Tsai Morris CH, Dufau ML.** Prolactin induces up-regulation of its cognate receptor in breast cancer cells via transcriptional activation of its generic promoter by cross-talk between ERα and STAT5. *Oncotarget* 5: 9079–9091, 2014. doi:10.18632/oncotarget.2376.

41. **LaPensee CR, Horseman ND, Tso P, Brandebourg TD, Hugo ER, Ben-Jonathan N.** The prolactin-deficient mouse has an unaltered metabolic phenotype. *Endocrinology* 147: 4638–4645, 2006. doi:10.1210/en.2006-0487.

42. **LeBaron MJ, Ahonen TJ, Nevalainen MT, Rui H.** In vivo response-based identification of direct hormone target cell populations using high-density tissue arrays. *Endocrinology* 148: 989–1008, 2007. doi:10.1210/en.2006-1219.

43. **Letexier D, Peroni O, Pinteur C, Beylot M.** In vivo expression of carbohydrate responsive element binding protein in lean and obese rats. *Diabetes Metab* 31: 558–566, 2005. doi:10.1016/S1262-3636(07)70231-8.

44. **Letexier D, Pinteur C, Large V, Fréring V, Beylot M.** Comparison of the expression and activity of the lipogenic pathway in human and rat adipose tissue. *J Lipid Res* 44: 2127–2134, 2003. doi:10.1194/jlr.M300235-JLR200.

45. **Ling C, Hellgren G, Gebre-Medhin M, Dillner K, Wennbo H, Carlsson B, Billig H.** Prolactin (PRL) receptor gene expression in mouse adipose tissue: increases during lactation and in PRL-transgenic mice. *Endocrinology* 141: 3564–3572, 2000.

46. **Ling C, Svensson L, Odén B, Weijdegård B, Edén B, Edén S, Billig H.** Identification of functional prolactin (PRL) receptor gene expression: PRL inhibits lipoprotein lipase activity in human white adipose tissue. *J Clin Endocrinol Metab* 88: 1804–1808, 2003. doi:10.1210/jc.2002-021137.

47. **Luque GM, Perez-Millán MI, Ornstein AM, Cristina C, Becu-Villalobos D.** Inhibitory effects of antivascular endothelial growth factor strategies in experimental dopamine-resistant prolactinomas. *J Pharmacol Exp Ther* 337: 766–774, 2011. doi:10.1124/jpet.110.177790.

48. **Matsumoto M, Ogawa W, Teshigawara K, Inoue H, Miyake K, Sakaue H, Kasuga M.** Role of the insulin receptor substrate 1 and phosphatidylinositol 3-kinase signaling pathway in insulin-induced expression of sterol regulatory element binding protein 1c and glucokinase genes in rat hepatocytes. *Diabetes* 51: 1672–1680, 2002. doi:10.2337/diabetes.51.6.1672.

49. **Meyre D, Delplanque J, Chèvre JC, Lecoeur C, Lobbens S, Gallina S, Durand E, Vatin V, Degraeve F, Proença C, Gaget S, Körner A, Kovacs P, Kiess W, Tichet J, Marre M, Hartikainen AL, Horber F, Potoczna N, Hercberg S, Levy-Marchal C, Pattou F, Heude B, Tauber M, McCarthy MI, Blakemore AI, Montpetit A, Polychronakos C, Weill J, Coin LJ, Asher J, Elliott P, Järvelin MR, Visvikis-Siest S, Balkau B, Sladek R, Balding D, Walley A, Dina C, Froguel P.** Genome-wide association study for early-onset and morbid adult obesity identifies three new risk loci in European populations. *Nat Genet* 41: 157–159, 2009. doi:10.1038/ng.301.

50. **Nadler ST, Stoehr JP, Schueler KL, Tanimoto G, Yandell BS, Attie AD.** The expression of adipogenic genes is decreased in obesity and diabetes mellitus. *Proc Natl Acad Sci USA* 97: 11371–11376, 2000. doi:10.1073/pnas.97.21.11371.

51. **Nagano M, Kelly PA.** Tissue distribution and regulation of rat prolactin receptor gene expression. Quantitative analysis by polymerase chain reaction. *J Biol Chem* 269: 13337–13345, 1994.

52. **Nanbu-Wakao R, Fujitani Y, Masuho Y, Muramatu M, Wakao H.** Prolactin enhances CCAAT enhancer-binding protein-beta (C/EBP beta) and peroxisome proliferator-activated receptor gamma (PPAR gamma) messenger RNA expression and stimulates adipogenic conversion of NIH-3T3 cells. *Mol Endocrinol* 14: 307–316, 2000.

53. **Nilsson L, Olsson AH, Isomaa B, Groop L, Billig H, Ling C.** A common variant near the PRL gene is associated with increased adiposity in males. *Mol Genet Metab* 102: 78–81, 2011. doi:10.1016/j.ymgme.2010.08.017.

54. **Nilsson LA, Roepstorff C, Kiens B, Billig H, Ling C.** Prolactin suppresses malonyl-CoA concentration in human adipose tissue. *Horm Metab Res* 41: 747–751, 2009. doi:10.1055/s-0029-1224181.

55. **Noaín D, Pérez-Millán MI, Bello EP, Luque GM, Casas Cordero R, Gelman DM, Peper M, Tornadu IG, Low MJ, Becú-Villalobos D, Rubinstein M.** Central dopamine D2 receptors regulate growth-hormone-dependent body growth and pheromone signaling to conspecific males. *J Neurosci* 33: 5834–5842, 2013. doi:10.1523/JNEUROSCI.5673-12.2013.

56. **Nogalska A, Sucajtys-Szulc E, Swierczynski J.** Leptin decreases lipogenic enzyme gene expression through modification of SREBP-1c gene expression in white adipose tissue of aging rats. *Metabolism* 54: 1041–1047, 2005. doi:10.1016/j.metabol.2005.03.007.

57. **Ouhtit A, Kelly PA, Morel G.** Visualization of gene expression of short and long forms of prolactin receptor in rat digestive tissues. *Am J Physiol* 266: G807–G815, 1994.

58. **Pala NA, Laway BA, Misgar RA, Dar RA.** Metabolic abnormalities in patients with prolactinoma: response to treatment with cabergoline. *Diabetol Metab Syndr* 7: 99, 2015. doi:10.1186/s13098-015-0094-4.

59. **Perez Millan MI, Luque GM, Ramirez MC, Noain D, Ornstein AM, Rubinstein M, Becu-Villalobos D.** Selective disruption of dopamine D2 receptors in pituitary lactotropes increases body weight and adiposity in female mice. *Endocrinology* 155: 829–839, 2014. doi:10.1210/en.2013-1707.

60. **Petryk A, Fleenor D, Driscoll P, Freemark M.** Prolactin induction of insulin gene expression: the roles of glucose and glucose transporter-2. *J Endocrinol* 164: 277–286, 2000. doi:10.1677/joe.0.1640277.

61. **Pi XJ, Grattan DR.** Increased expression of both short and long forms of prolactin receptor mRNA in hypothalamic nuclei of lactating rats. *J Mol Endocrinol* 23: 13–22, 1999. doi:10.1677/jme.0.0230013.

62. **Ramirez MC, Ornstein AM, Luque GM, Perez Millan MI, Garcia-Tornadu I, Rubinstein M, Becu-Villalobos D.** Pituitary and brain dopamine D2 receptors regulate liver gene sexual dimorphism. *Endocrinology* 156: 1040–1051, 2015. doi:10.1210/en.2014-1714.

63. **Rui L.** Energy metabolism in the liver. *Compr Physiol* 4: 177–197, 2014. doi:10.1002/cphy.c130024.

64. **Saltiel AR, Kahn CR.** Insulin signalling and the regulation of glucose and lipid metabolism. *Nature* 414: 799–806, 2001. doi:10.1038/414799a.

65. **Sauvé D, Woodside B.** Neuroanatomical specificity of prolactin-induced hyperphagia in virgin female rats. *Brain Res* 868: 306–314, 2000. doi:10.1016/S0006-8993(00)02344-1.

66. **Serri O, Li L, Mamputu JC, Beauchamp MC, Maingrette F, Renier G.** The influences of hyperprolactinemia and obesity on cardiovascular risk markers: effects of cabergoline therapy. *Clin Endocrinol (Oxf)* 64: 366–370, 2006. doi:10.1111/j.1365-2265.2006.02469.x.

67. **Shimano H, Shimomura I, Hammer RE, Herz J, Goldstein JL, Brown MS, Horton JD.** Elevated levels of SREBP-2 and cholesterol synthesis in livers of mice homozygous for a targeted disruption of the SREBP-1 gene. *J Clin Invest* 100: 2115–2124, 1997. doi:10.1172/JCI119746.

68. **Sorenson RL, Brelje TC, Hegre OD, Marshall S, Anaya P, Sheridan JD.** Prolactin (in vitro) decreases the glucose stimulation threshold, enhances insulin secretion, and increases dye coupling among islet B cells. *Endocrinology* 121: 1447–1453, 1987. doi:10.1210/endo-121-4-1447.

69. **Soukas A, Socci ND, Saatkamp BD, Novelli S, Friedman JM.** Distinct transcriptional profiles of adipogenesis in vivo and in vitro. *J Biol Chem* 276: 34167–34174, 2001. doi:10.1074/jbc.M104421200.

70. **Strain AJ, Ingleton PM.** Growth hormone- and prolactin-induced release of insulin-like growth factor by isolated rat hepatocytes. *Biochem Soc Trans* 18: 1206, 1990. doi:10.1042/bst0181206.

71. **Topping DL, Mayes PA.** The immediate effects of insulin and fructose on the metabolism of the perfused liver. Changes in lipoprotein secretion, fatty acid oxidation and esterification, lipogenesis and carbohydrate metabolism. *Biochem J* 126: 295–311, 1972. doi:10.1042/bj1260295.

72. **Uyeda K, Repa JJ.** Carbohydrate response element binding protein, ChREBP, a transcription factor coupling hepatic glucose utilization and lipid synthesis. *Cell Metab* 4: 107–110, 2006. doi:10.1016/j.cmet.2006.06.008.

73. **Viengchareun S, Bouzinba-Segard H, Laigneau JP, Zennaro MC, Kelly PA, Bado A, Lombès M, Binart N.** Prolactin potentiates insulin-stimulated leptin expression and release from differentiated brown adipocytes. *J Mol Endocrinol* 33: 679–691, 2004. doi:10.1677/jme.1.01563.

74. **Wang Y, Viscarra J, Kim SJ, Sul HS.** Transcriptional regulation of hepatic lipogenesis. *Nat Rev Mol Cell Biol* 16: 678–689, 2015. doi:10.1038/nrm4074.

75. **White UA, Stephens JM.** Transcriptional factors that promote formation of white adipose tissue. *Mol Cell Endocrinol* 318: 10–14, 2010. doi:10.1016/j.mce.2009.08.023.

76. **Wittmann G, Liposits Z, Lechan RM, Fekete C.** Medullary adrenergic neurons contribute to the neuropeptide Y-ergic innervation of hypophysiotropic thyrotropin-releasing hormone-synthesizing neurons in the rat. *Neurosci Lett* 324: 69–73, 2002. doi:10.1016/S0304-3940(02)00165-9.

77. **Yahagi N, Shimano H, Hasty AH, Matsuzaka T, Ide T, Yoshikawa T, Amemiya-Kudo M, Tomita S, Okazaki H, Tamura Y, Iizuka Y, Ohashi K, Osuga J, Harada K, Gotoda T, Nagai R, Ishibashi S, Yamada N.** Absence of sterol regulatory element-binding protein-1 (SREBP-1) ameliorates fatty livers but not obesity or insulin resistance in Lep(ob)/Lep(ob) mice. *J Biol Chem* 277: 19353–19357, 2002. doi:10.1074/jbc.M201584200.

78. **Yamashita H, Takenoshita M, Sakurai M, Bruick RK, Henzel WJ, Shillinglaw W, Arnot D, Uyeda K.** A glucose-responsive transcription factor that regulates carbohydrate metabolism in the liver. *Proc Natl Acad Sci USA* 98: 9116–9121, 2001. doi:10.1073/pnas.161284298.

79. **Yavuz D, Deyneli O, Akpinar I, Yildiz E, Gözü H, Sezgin O, Haklar G, Akalin S.** Endothelial function, insulin sensitivity and inflammatory markers in hyperprolactinemic pre-menopausal women. *Eur J Endocrinol* 149: 187–193, 2003. doi:10.1530/eje.0.1490187.